Queensland University of Technology
Brisbane Australia

This may be the author's version of a work that was submitted/accepted for publication in the following source:

Khan, Md Imran Hossen & Karim, Azharul
(2017)
Cellular water distribution, transport, and its investigation methods for plant-based food material.
Food Research International, *99*(1), pp. 1-14.

This file was downloaded from: https://eprints.qut.edu.au/108223/

© Consult author(s) regarding copyright matters

This work is covered by copyright. Unless the document is being made available under a Creative Commons Licence, you must assume that re-use is limited to personal use and that permission from the copyright owner must be obtained for all other uses. If the document is available under a Creative Commons License (or other specified license) then refer to the Licence for details of permitted re-use. It is a condition of access that users recognise and abide by the legal requirements associated with these rights. If you believe that this work infringes copyright please provide details by email to qut.copyright@qut.edu.au

License: Creative Commons: Attribution-Noncommercial-No Derivative Works 2.5

Notice: *Please note that this document may not be the Version of Record (i.e. published version) of the work. Author manuscript versions (as Submitted for peer review or as Accepted for publication after peer review) can be identified by an absence of publisher branding and/or typeset appearance. If there is any doubt, please refer to the published source.*

https://doi.org/10.1016/j.foodres.2017.06.037

Cellular Water Distribution, Transport, and Its Investigation Methods for Plant-Based Food Material

Md. Imran H. Khan[1, 2], M.A. Karim[*1]

[1]Science and Engineering Faculty, Queensland University of Technology (QUT),

2 George St, Brisbane, QLD 4000, Australia

[2]Department of Mechanical Engineering, Dhaka University of Engineering & Technology,

Gazipur-1700, Bangladesh

[*]Email : azharul.karim@qut.edu.au ; Phone : +

Abstract

Heterogeneous and hygroscopic characteristics of plant-based food material make it complex in structure, and therefore water distribution in its different cellular environments is very complex. There are three different cellular environments, namely the intercellular environment, the intracellular environment, and the cell wall environment inside the food structure. According to the bonding strength, intracellular water is defined as loosely bound water, cell wall water is categorized as strongly bound water, and intercellular water is known as free water (FW). During food drying, optimization of the heat and mass transfer process is crucial for the energy efficiency of the process and the quality of the product. For optimizing heat and mass transfer during food processing, understanding these three types of waters (strongly bound, loosely bound, and free water) in plant-based food material is essential. However, there are few studies that investigate cellular level water distribution and transport. As there is no direct method for determining the cellular level water distributions, various indirect methods have been applied to investigate the cellular level water distribution, and there is, as yet, no

consensus on the appropriate method for measuring cellular level water in plant-based food material. Therefore, the main aim of this paper is to present a comprehensive review on the available methods to investigate the cellular level water, the characteristics of water at different cellular levels and its transport mechanism during drying. The effect of bound water transport on quality of food product is also discussed. This review article presents a comparative study of different methods that can be applied to investigate cellular water such as nuclear magnetic resonance (NMR), bioelectric impedance analysis (BIA), differential scanning calorimetry (DSC), and dilatometry. The article closes with a discussion of current challenges to investigating cellular water.

Keywords: bound water, free water, NMR, DSC, BIA

1. Introduction

Food materials, specifically plant-based foods, are complex in nature as they have heterogeneous, hygroscopic and porous properties that contain up to 80–90 % water (Khan, Kumar, Joardder, & Karim, 2017a). This vast amount of water is located in different cellular environments inside the food structure. According to biological analysis, the vacuole, cytoplasm, cell wall and extracellular space are the main cellular locations in food tissue that contain this water in differing proportions (Aguilera & Stanley, 1999). Food thermal processing (drying, frying, and cooking) researchers have found that the water in food tissue mainly exists in three different cellular environments, namely intercellular space, intracellular space, and the cell wall environment (Khan, Joardder, Kumar, & Karim, 2016a). The intercellular spaces or environments are those where some unrestricted spaces have been made by the connection of two or more cells as shown in Figure 1. These unrestricted spaces are mostly composed of air, a small portion of water, and other solutes (such as sugar). The small portion of water that is contained in this space is termed intercellular water or simply free water (FW). The vacuole and cytoplasm together are considered as intracellular spaces that act as a water reservoir in fruit tissue. Generally, the water that resides in this area is known as intracellular water. The water held in the microspace in a cell wall environment is sometimes referred as extracellular water (L. Van Der Weerd, Claessens, Efdé, & Van As, 2002) or cell wall water. The waters in different cellular environments have different bonding capacities. According to their bonding strength, some waters are referred as bound water (see section 2). Understanding the proportions of water occupying different cellular environments in plant-based food tissue is crucial for optimizing energy consumption and obtaining better quality of dried foods during food drying (Khan et al., 2016b). However, the proportions of different cellular waters, transport mechanisms, and the effect of bound water transport on food quality have not been widely reported in the available literature to date. To obtain a better understanding of how

cellular water moves from one cellular environment to another cellular environment as well as their effect on food quality, extensive experimentation is needed.

There are several methods that can potentially be used for measuring the different types of water, including differential scanning calorimetry (DSC), differential thermal analysis (DTA), dilatometry, bioelectric impedance analysis (BIA), and nuclear magnetic resonance (NMR). Due to the specific limitations of the various methods, they may not be equally suitable for the application in plant-based food tissue for measuring cellular level water (Khan et al., 2016b).

[Figure 1 can be inserted here]

Therefore, the primary aim of this article is to present a comprehensive review of various methods for measuring cellular water and identify which method is best for plant-based food material. It is also the objective of the present work to a provide a comprehensive review of the characteristics of different types of cellular water and their transportation mechanisms, their effect on the food properties during food drying, and consideration of cellular water transport in existing drying models. This article is organized as follows. First, a clear explanation of the different types of cellular water and their classification with their characteristics is presented. Second, the transport mechanism of cellular water and its consideration of transport in existing food drying models are clearly explained. Third, a comprehensive review of different methods (NMR, DSC, BIA, DIL) that can be used for measuring cellular waters is presented. Then the current status of research on cellular water distribution in food tissue is discussed. The article closes with discussion of a major challenge to the measurement of cellular water distribution and transport.

1.1 Classification of cellular water and its characteristics

In cellular tissue, water is distributed in different cellular environments in different proportions according to their macromolecular bonding strength, and therefore they are categorized by terms and definitions that reflect their diverse characteristics, as discussed below.

Bound water is the water that is physically trapped within a restricted environment and therefore is hard to transport during food drying (Khan et al., 2016a). Bound water can be defined as the proportion of water in various materials (such as animal and plant cells or soils) that are associated with the colloid phase with strong micromolecular binding strength (Caurie, 2011). In plant-based food material, water can be bound physically and chemically. The water that resides in intracellular environment, and cell wall environment is categorized as physically bound water (Joardder, Brown, Kumar, & Karim, 2017; Karel & Lud, 2003). A very small amount of water bonded with the chemical (nutrition) is categorized as chemically bound water. The chemically bound water should not be considered for transport due to its great impact on the taste and flavor of the dried food (Kuprianoff, 1958). Therefore, physically bound water is the main concern for transport during food processing.

Physically bound water can be divided into two different categories based on its micromolecular bonding strength: loosely bound water (LBW) and strongly bound water (SBW); intracellular water is LBW and cell wall water is SBW (Caurie, 2011; Khan et al., 2016b). These two types of water (LBW and SBW) are sometimes referred to as the monolayer water and multilayer water respectively (Rockland, 1969), or as vicinal water and constitutional water (Yamsaengsung & Moreira, 2002).

Sometimes bound water can be defined based on its physical characteristics. The physical characteristics of bound water are different from FW**. Free water is located in the pores and the capillaries and can easily be removed during drying. One of the major**

characteristics of FW is that it diffuses faster than bound water (Khan et al., 2016a). Yamsaengsung and Moreira (2002) argue that the enthalpy of vaporization of SBW is much greater than that of pure water. This water forms a monolayer over the hydrophilic region of the solid material by either water–ion or water–dipole interaction. Moreover, in food material, LBW is associated with neighboring molecules mainly by water-water and water-solute hydrogen bonding (Yamsaengsung & Moreira, 2002). **Based on the consideration of the water mobility, the LBW has the lower diffusivity than FW.** Therefore, the variation in binding energy of bound water strongly affects the drying process, since it requires more energy than FW (Shafiur, 2007). Furthermore, it is reported that bound water (SBW) is not free to act as a solvent for salts and sugars (Vaclavik & Christian, 2008). It can be frozen only at very low temperatures (below the freezing point of normal water), it exhibits essentially no vapor pressure, and its density probably greater than that FW (Vaclavik & Christian, 2008). Based on these characteristics, Briggs (1932) argued that bound water is the proportion of water in a system associated with the colloid phase with such strength that it is no longer available to act as a solvent or to be separated from the colloid phase by freezing, because they are prevented from separating from the nonwater constituents and other substances by high heats of adsorption. Thus, it can be argued that the physical characteristics of bound water are not similar to that of FW and therefore the transport properties (for instance, diffusivity) of bound water will differ from FW.

1.2 Transport mechanism of cellular water during drying

The mechanisms of heat and mass transfer in a food material depend on the physical structure and the chemical composition of that material. Hygroscopic food material contains three types of water: SBW, LBW, and FW as discussed above. SBW is tightly held in the cell wall environment and therefore cannot be transported during thermal processing. The latter

two types of water are the main concern during thermal processing (Khan et al., 2016a). The transport mechanism of FW and LBW may be different due to their diverse transport properties. FW can migrate from intercellular spaces to the surface by diffusion and convection where it can be removed by evaporation from the surface to the environment air (Srikiatden & Roberts, 2007). Studies of the transport mechanism of LBW are inadequate and unclear (Feng, Tang, Cavalieri, & Plumb, 2001). Turner, Puiggali, and Jomaa (1998) assumed that bound water transfer was caused by only diffusion while others postulated a capillary mechanism to characterize bound water flow (Peishi & Pei, 1989). Feng et al. (2001) hypothesized that a universal driving force that comes from the chemical potential gradient is responsible for migrating LBW. It has also been hypothesized that bound water is removed by progressive vaporization within the solid matrix, followed by diffusion and pressure-driven transport of water vapor through the solid (Datta, 2007).

Therefore, the transport mechanism of LBW is still an unsolved issue for food processing. It can be assumed that LBW (intracellular water) can migrate in two ways: First, migration from intracellular spaces to the intercellular spaces after rupturing the cell membrane (Halder, Datta, & Spanswick, 2011), a phenomenon defined as apoplastic transport. Second, LBW can migrate from cell to cell through very fine capillaries (micro-channels) (Feng et al., 2001), and it is referred to as symplastic transport. However, the physics behind these two types of transport is still not clearly understood. Halder et al. (2011) investigated the effect of temperature on LBW transport during thermal processing of food material. They argued that LBW migrated through rupturing of the cell membrane at or above 50°C. According to their argument, all of the membranes of the cell collapse at once after reaching a specific temperature during processing. However, their argument is not justified because cell collapse depends on internal thermal stress (Prothon, Ahrne, & Sjoholm, 2003) that first develops near the surface and gradually penetrates to the center of the sample during convective drying. As a result, the

cells may collapse progressively from the surface to center (Srikiatden & Roberts, 2007). **Khan, Wellard, Joardder, and Karim (2017b) investigated the cellular water transport phenomena using ^{1}H-NMR T_2 relaxometry during drying. They found that LBW migrates from intracellular region to the intercellular environment through rupturing the cell membrane. They argued that cell membranes rupture at different stages of drying rather than collapsing at one time. Moreover, they postulated that most of the cell membranes rupture at the middle stage of drying. This argument is in disagreement with the findings of Halder et al. (2011) discussed above.**

Therefore, from the above discussion, it can be argued that the migration mechanism of bound water is not yet clearly understood; however, it is crucial to know the fundamental mechanism of bound water transport during thermal processing of food material in order to optimize energy consumption and achieve better quality during food drying.

1.3 Effect of bound water transport on food properties during thermal processing

The structural heterogeneity of food material makes the transport of water during thermal processing complex. Transport of cellular water (LBW and SBW) greatly affects the food quality by deforming its physical structure (shrinkage), or changing its texture, color, or nutritional properties. During food processing, materials change their structure due to uneven material shrinkage. When LBW or SBW is migrated, microstructural stress may be induced due to the moisture gradient within the product that leads to shrinkage. **Figure 2 shows the effect of different types of cellular water transport on material shrinkage during drying. It can be seen that trasnport of FW has no effect on shrinkage whereas migration of LBW contributes to cellular shrinkage, pore formation, and collapse of the cells. Overall food tissue is deformed due to the migration of SBW (Figure 2) (Joardder, Karim, Brown, and Kumar 2015). This hypothesis is justified by Khan et al. (2017b). They found that the**

LBW is migrated from interacellular environment to the intercellular region thorugh rupturing the cell membrane during drying. They also argued that cell membrane rupture progressively at different stages of drying (Figure 2) rather than collapsing at once. Prothon et al. (2003) showed that migration of three types of water causes overall tissue shrinkage and cellular shrinkage as well as structure collapse. Vicente, Nieto, Hodara, Castro, and Alzamora (2012) found changes in quantity of LBW strongly affect the cell deformation during osmotic dehydration. They argued that LBW exerts an overpressure on the cell membrane and leads to propagate cell collapse during osmotic dehydration. Khan et al. (2016b) developed a relationship between FW and porosity. They argued that transport **of cellular water** strongly affect the porosity of the material, while transport of SBW depends on the proportion of solid material content in different food tissue. Moreover, transport of SBW leads to the overall tissue collapse.

Watercore is a physiological disorder of a fruit tissue that is characterized by water-soaked tissue around the vascular bundles or core area due to the spaces between cells becoming filled with fluid instead of air (Dart and Newman, 2005). Affected tissue is water-soaked and glassy looking. Generally, this damage cannot possible to see from the outer side of the tissue. This damage is only appeared while fruits are cut. In severe cases flesh can be affected right up to the skin, which then darkens over affected areas. Many researchers have investigated the effect of LBW and SBW during the development of the watercore (Cho, Chayaprasert, & Stroshine, 2008; Clark, MacFall, & Bieleski, 1998; Melado-Herreros et al., 2013), internal browning **(caused by low-temperature storage in certain apple varieties)** (Cho et al., 2008; Clark & Burmeister, 1999; J. J. Gonzalez et al., 2001), and microstructural heterogeneity (Defraeye et al., 2013; Winisdorffer et al., 2015) in apple tissue. Most of the studies found that development of internal browning and water core mainly depends on the water mobility in different cellular environments. However, studies of the effect

of bound water on quality assurance during thermal processing are very limited, and there is clearly a need for more study of the transport of bound water and its effect on food quality.

[Figure 2 can be inserted here]

1.4 Consideration of bound water transport in food drying models

There are many models that have been developed for thermal processing like drying, frying, cooking, and baking of food materials. Existing food processing models can be categorized as empirical, single-phase, and multiphase models. The empirical models are suited for a specified product and processing condition and therefore cannot be used for even a slightly different situation, while the single-phase model is not much better. During single-phase modeling, all the water in food material is considered as bulk water that can be transported by diffusion (Khan et al., 2017). Although many single-phase models have been developed and good agreement with experimental results been found, these models are oversimplified and do not consider the fundamental physics of food processing (Khan et al., 2016a). In contrast, a multiphase model considers the transport mechanisms of liquid water, water vapor, and air separately. Multiphase models are more comprehensive and provide better insight into the transport mechanisms, because they can account for temporal and spatial profiles of temperature, liquid water, water vapor, and air inside the food material. A detailed outline of existing multiphase models for food processing can be found in the literature (Khan et al., 2016a), where the limitations of (or gaps in) existing food processing models have been presented clearly. The main limitation of the current food processing models is that transport of bound water has not been taken into consideration for modeling. Most of the existing multiphase models have considered all of the water inside the food materials to be transportable (i.e., as bulk water). Although this simplistic assumption makes the problem easier to

formulate, it does not incorporate a realistic understanding of heat and mass transfer during food processing.

Some researchers have attempted to develop a multiphase model that considers the transport of bound and free waters separately for the drying of wood (Skaar & Babiak, 1982; Turner et al., 1998), food (Feng et al., 2001; Peishi & Pei, 1989), and sludge (Lee & Lee, 1995). These models have been developed based on some simplified assumptions, including the assumption that bound water can be transported only through diffusion (Turner et al., 1998); however, movement of bound water cannot be simply described by a diffusion process (discussed in section 2.1). Peishi and Pei (1989) developed a multiphase model considering bound water transport. They posited that LBW moves through the semipermeable membranes along the array of the cellular structure through capillary diffusion and that for granular porous materials the bound water moves along very fine capillaries. These assumptions conflict with the findings of Halder et al. (2011) (as discussed in section 2.1). Peishi and Pei (1989) argued that migration of LBW is caused by a moisture gradient. However, LBW migrates during cell membrane collapse due to temperature gradient (Halder et al., 2011) although moisture has some small influence for migrating LBW. Feng et al. (2001) developed a multiphase model that considered bound water transport for drying apple, but the physics behind the bound water transport was not explained clearly although they included mass flux equation for bound moisture transport. Based on the sorption isotherm process, bound water remains attached with the solid material, and it can be expressed by a sorption equilibrium diagram. Sometimes it is assumed that bound water may be transported through sorption diffusion or “liquid moisture transfer near dryness”. Based on this assumption much research has been conducted to develop a model for the drying of granular materials (Bramhall, 1979; Whitaker & Chou, 1983). Although these studies show some good agreement, the transport of bound water has not been explained clearly and realistically. Because of the limited understanding of bound water

transport during food processing, the existing model only considers some simplistic assumptions regarding the transport of bound water during thermal processing. Therefore, a fuller, more realistic understanding of the mechanism of bound water transport is needed for developing accurate physics-based food process modeling. To obtain a better understanding of how cellular water moves from one cellular environment to another cellular environment, extensive experimentation is needed. Several methods have been proposed to measure the cellular waters. However, not all methods are suitable for measuring cellular water in food tissue. The following section discusses some suitable methods and their limitations for investigating the cellular level water in different biological tissues.

2. Methods of investigating cellular water

The exact definition of bound water depends on the method used for its determination (Kuprianoff, 1958). During the past two decades, a variety of technologies have been evaluated for their potential to nondestructively determine the cellular water environment and quality of fruits and vegetables (Abbott, Lu, Upchurch, & Stroshine, 2010). However, not all methods are suitable for investigating the cellular waters in food material. Some suitable methods to investigate cellular water are discussed below.

2.1 Differential scanning calorimetry (DSC)

2.1.1 Theory

Most of the foods material contains about 80-90% water that exist in different cellular environment (discussed in section 1.1). This vast amount of water has three phase transitions in the temperature range of interest: crystallization on cooling or ice melting on heating, vaporization (or condensation), and sublimation. The melting and

vaporization of water depends on its associated specific enthalpy under atmospheric pressure. These two phenomena are refereed as endothermic process which is easily observed using DSC. A differential scanning calorimeter is a thermodynamic tool that determines the temperature and heat flow associated with material transitions as a function of time and temperature (Gill, Moghadam, & Ranjbar, 2010). During a change in temperature, the calorimeter measures the heat that is radiated or absorbed by the sample using of the temperature difference between the sample and the reference material (Haines, Reading, & Wilburn, 1998). For DSC analysis, it is assumed that the FW in hygroscopic food material melts at a specific temperature and that the transition temperature, enthalpy, and peaks in DSC curves (Figure 3) are the same as for pure water (Nakamura, Hatakeyama, & Hatakeyama, 1981). The water with a melting point below a specific temperature is assumed as bound water, which is restricted by its macromolecular content and the transition is not detected in the first-order transition (Nakamura et al., 1981). In a heat flux DSC, a well-defined heat conduction path of known thermal resistance is used for the heat exchange of the sample to be measured. The primary signal is a temperature difference between a sample and a reference. The instrument determines the temperature and heat flow associated with material phase transitions as functions of time and temperature (Peyronel & Marangoni, 2014). Physical phenomena studied with DSC include glass transitions, melting profiles, heats of fusion, amount of crystallinity, oxidative stability, curing kinetics, crystallization kinetics, and other phase transitions**. The DSC process can be subdevided in two categories. The first category is the exothermic process where the heat energy released from the system to the surroundings. This proces is usually used for the investigation of the material decomposition and crystalisation. The second type of endothermic process is that which absobs energy into the system. For example, in pahse transitions the heat is absorbed and therefore heat flow**

to the sample is higher than that to the reference. The endothermic process is used to analyse the glass transitions, melting profiles, and heats of fusion in samples.

[Figure 3 can be inserted here]

2.1.2 Working procedure during DSC

Proper sample preparation is essential to obtain significant data from DSC. The sample preparation involves the encapsulation of the material in pans designed for DSC analysis. In measuring the weights of empty pan and the sample, software can be used in DSC which gives accurate measurements. It is important to accurately measure these values so that the transition enthalpy can correctly be reported. The sample should be placed directly in the hermetic aluminum pan because transferring the sample from weighing paper to the pan can lead to a loss of material. During filling the pan, proper care should be taken to avoid the overfilling which may cause sample spills when the pan is being sealed. Overfilled and leaking pans will lead to erroneous readings and most critically, contamination of the cell. The sealed sample pan and reference pan should then be placed on the heat source slot. Application software (such as TA Universal Analysis on the desktop computer) can be used for analyzing the thermal effects (endothermic and exothermic). The following mathematical analysis can be then performed to calculate the free and bound water in biological tissues.

Mathematical analysis: When the differential scanning calorimeter is used in scanning mode, the temperature changes in a linear fashion. The heat flow rate, Q, is proportional to the heating rate dT/dt, with K as the proportionality factor.

$$Q = K\frac{dT}{dt} \quad (1)$$

where *T* is temperature (^{o}C), and *t* is time (sec). In DSC, the differential heat flow rate depends on the differential heat capacity between the pan containing the sample and the reference pan (which is usually empty) and the heating rate. The measured heat flow in scanning mode is never zero and is made up of three parts:

$$Q(T,t) = Q_o(T) + Q_{cp}(T) + Q_r(T,t) \quad (2)$$

Where Q_o is due to the difference in temperature between the sample and reference positions, Q_{cp} is due to the difference in heat capacity between sample and reference, and Q_r is the heat flow contribution from the latent heat of transition in the sample. The first and second terms define the baseline, and the third term defines the peak of the measured curve, as shown in Figure 3.

It can be seen from the DSC curve (Figure 3) that there are two peaks: peak I and peak II. **The rate of absorption of heat energy during DSC experiment can be expressed by these two endothermic peaks. These two peaks result from the enthalpy associated with the change in water phase and differences in water mobility (Peyronel & Marangoni, 2017). The first endothermic peaks (Peak II) refers to solid state phase transition of the crystalline material compound and the second peak (peak I) refers to the melting point of the material with an onset temperature and a peak temperature. The area of this melting peak increases as the percent of crystallinity of the material increases. This small peak is then shifted to a higher temperature range with the increase of certain amount of water, and then reached an upper temperature limit (peak I). The heat of crystallization for peak II also increased in the initial stage and then attained a constant value. A new sharp peak (peak I) appears when the amount of water in each sample exceeds that needed to show a constant heat of crystallization for peak II (Hatakeyama, Nakamura, &**

Hatakeyama, 1988). During DSC experimentation, this certain amount of additional water must be added to the sample to increase the enthalpy of freezing and the following equation is used.

$$W_l = W_1 + W_2 + W_{nf} \quad (3)$$

$$W_l = W_m + W_{nf} \quad (4)$$

Where W_l is the total weight of water added to the sample, W_1 and W_2 are the weights of water calculated from the enthalpy of peak I and peak II, respectively (**Figure 3**), W_{nf} is the weight of nonfreezing water, and W_m is the weight of water that can be calculated from the melting enthalpy.

The bound water can be calculated from the following **equation, where W_s is the total weight of the sample and W_b is the weight of bound water**

$$\%BW = \left(\frac{W_b}{W_s}\right) \times 100 \quad (5)$$

$$W_b = W_2 + W_{nf} \quad (6)$$

Then the proportion of free and bound water can be calculated from the following equation.

$$FW = 1 - BW \quad (7)$$

where BW is the bound water, FW is the free water, and W_s is the **total** weight of the sample.

2.1.3 Current status of DSC application in biological tissue analysis

Many studies have been conducted using DSC to find the bound water content in polymers (Hatakeyama, Nakamura, & Hatakeyama, 1988; Tatsuko Hatakeyama, Tanaka, Kishi, & Hatakeyama, 2012; Ohno, Shibayama, & Tsuchida, 1983), sludge (Lee & Hsu, 1995), carboxymethylcellulose (Nakamur, Minagaw, Hatakeyam, & Hatakeyama, 2004), cotton,

kapok, linen, jute, wood (Nakamura et al., 1981), and beef (Aktaş, Tülek, & Gökalp; Schwartzberg, 1976). By contrast, the literature on the application of DSC to investigate bound and free water in plant-based materials is very limited, although some reports describe the investigation of the relationship between quality and water distribution (Goñi, Fernandez-Caballero, Sanchez-Ballesta, Escribano, & Merodio, 2011; Kerch, Glonin, Zicans, & Meri, 2012**). Based on the freezing and non-freezing temperatures effect on the structural dysfunctions, many research works have been done, mainly focused on the membrane integrity loss, membrane rigidification, and changes in cell wall properties (Yamada et al., 2002; Kratsch & Wise, 2000). It is argued that the change of cell wall composition and properties in fruits are associated with storage at low temperature (Bauchot, Hallett, Redgwell, and Lallu, 1999).**

2.1.4 Limitations of DSC

During DSC analysis of cellular water in plant-based food tissue, it is assumed that the FW in hygroscopic food material melts at a specific temperature (Nakamura et al., 1981), and water with a melting point below that temperature is the bound water. With this assumption, it is easier to investigate the intercellular water (FW) and intracellular water (LBW) in plant-based food material. However, it might not be possible to find SBW in this method. Moreover, **DSC is suitable to investigate subcellular water changes during freeze drying. It may not possible to use DSC with a hot air drying setup due to the temperature limitations. Therefore, researcher can use DSC as a perfect tool who would like to investigate different cellular water distribution during freeze drying. Beside this, DSC can be used as a unique tool for studying the relationship of water content associated with qualitative information in diverse food material rather than quantitative information (Khan et al. 2016b).**

2.2 Bioelectrical impedance analysis (BIA)

2.2.1 Theory

BIA is a very simple and established technique for measuring body composition. It measures the resistance of tissues to the flow of electrical current. The proportion of different components in tissue can be calculated because current flows more easily through the parts of the material that are composed mostly of water. The current passes between two electrodes, often called the source and sink (or detector), and generates voltages between different points in the body volume according to Ohm's law. The current flows through all conducting material present in the body in the path between the source and sink electrodes. Because living tissue constitutes a volume conductor, the physical carriers of the current are predominantly charged ions, such as sodium or potassium ions, which can move within the volume. Conductivity within such materials is high where the water density and its intensity are low. In plant-based food tissue, low density water ions are present in intercellular spaces **that are defined by** R_1. In intracellular spaces, water is present with vitamins and minerals as a mixer and therefore its density is higher (Khan et al., 2016a), the resistance in intracellular spaces are **difined** by R_2 as shown in Figure 4. On the other hand, the cell wall environment in food tissue is largely of chemical composition and water molecules are very rare; therefore, the density of the cell wall is mostly higher than other two (intercellular and intracellular) environments. Current will flow predominantly through materials with higher conductivities, as shown in Figure 4 (a). There is a lower resistance to current flow in regions where the conductor has a larger cross-sectional area and fewer obstacles, such as cell membranes, that form barriers to charge movement (Figure 4).

The actual parameter measured with BIA is the voltage (V) that is produced between two electrodes located most often at sites near to, but different from, the sites where current is

introduced. The measurement is usually expressed as a ratio, *V/I*, also called impedance (*Z*). The measuring instrument is therefore called a bioelectrical impedance analyzer. Impedance (*Z*) has two components, resistance (*R*) and reactance (*X*). A plot of reactance (*X*) versus resistance (*R*) of a tissue for various frequencies is known as a Cole–Cole plot, as shown in Figure 5.For complicated plant tissues, the tissue is better modeled by the impedance level Cole–Cole function (Zhang, Repo, Willison, & Sutinen, 1995) as described in Equation (12)

$$Z = R_{\infty} + \frac{R_o - R_{\infty}}{1 + (j\omega T_c)^{(1-\alpha)}} \quad (8)$$

In this relationship, R_o is the impedance measured at low frequency that corresponds to extracellular resistance, T_c is a generalized time constant, j is an imaginary unit, ω is the angular frequency, and α is the Cole–Cole function where the range of α is 0–1. R_{∞} is the resistance at extremely high frequency and it is the best theoretical value of impedance due to the extracellular and intracellular fluid.

[Figure 4 can be inserted here]

[Figure 5 can be inserted here]

It can be noted that the reactance component of impedance vector is zero at high frequency (R_{∞}) because the current flow at this frequency is not be affected by interaction with the cell membranes and that it will pass directly through the cell membranes (Halder et al., 2011). Therefore, R_{∞} can be calculated from the following equation

$$R_{\infty} = \frac{R_1 R_2}{R_1 + R_2} \quad (9).$$

To obtain a better understanding for the application of BIA in food tissue, readers should refer to Halder, Datta and Spanwick's recent publication (Halder et al., 2011).

2.2.2 BIA working procedure

When conducting BIA, a body composition meter must be used. There are many types of body composition meters available in the market**. Two-terminal auto Balance Bridge with digital calibration (Diao et al., 2012) is an amenable technique for integration in implantable devices since it requires only two electrodes. This technique is quite simple and easy and therefore this technique is commonly used for most of the biological tissue analysis. However, this method has the drawback that it measures the interface electrode impedances which can be much larger than the tissue's impedance. Therefore, an inaccurate result can be obtained. On the other hand, four terminal electrode methods are the most significant and latest techniques that can be used for investigating different types of water in biological tissue. The main advantage of this type of tetrapolar bio-impedance spectroscopy is that it can reduce the non-ideal effects of the electrode polarization impedance. However, tetrapolar measurements include errors from electrode placement and negative sensitivity regions within the typical region of interest beneath the electrodes (Grimnes & Martinsen, 2007).** The IMP SFB7 body composition meter (Impedimed, San Diego, CA) can be used for plant tissue analysis (Halder et al., 2011). It is a tetrapolar bio-impedance spectroscopy device with a single channel that can scan 256 frequencies between 4 and 1000 kHz for the estimation of impedances in tissues. Before beginning the measurement, the equipment should be calibrated using the provided calibration cell. Needle electrodes should be placed inside opposite ends of the same side of a prepared sample, as shown in Figure 6. Then electric current should be supplied and the impedance data from the impedance analyzer recorded. Using this impedance data intracellular water can be

calculated from the following equation (Eqn.10) (De Lorenzo, Andreoli, Matthie, & Withers, 1997). Detailed experimental procedures have been published elsewhere (Cox, Zhang, & Willison, 1993; Dejmek & Miyawaki, 2002; Zhang MIN, 1990).

$$1+\left(\frac{V_2}{V_1}\right)^{5/2}=\frac{R_1+R_2}{R_2}\left(1+\kappa\frac{V_2}{V_1}\right) \tag{10}$$

In this relationship, V_2 is intracellular water volume, V_1 is the intercellular water volume. The parameter κ is the ratio of electrical resistivity in intracellular fluid to electrical resistivity in extracellular fluid, and has been determined for animal cells to be between 3.2 and 3.71 (De Lorenzo, Andreoli, Matthie, & Withers, 1997).

[Figure 6 can be inserted here]

2.2.3 BIA application

For a wide range of biological tissue analysis, it is well established that the Cole–Cole function provides a better fit and thus many researchers have examined morphological behavior in different biological tissues, for instance, the level of injury due to freeze thaw cycles in potato (Zhang MIN, 1990), estimating the extent of bruising in apples (Cox et al., 1993), assessing the maturity of nectarines (Dejmek & Miyawaki, 2002), and examining the effect of drying and freezing-thawing treatments on eggplants, tubers, and carrots (Wu, Ogawa, & Tagawa, 2008).

BIA has the advantage that it is simple and nondestructive, and it can be used for measuring water distribution in biological tissue. Some studies have used this technique to find the intracellular and extracellular water in animal tissue (Dean, Ramanathan, Machado, &

Sundararajan, 2008; Webber & Dehnel, 1968). **Few researchers used this technique to investigate different cellular water in plant-based food material. Halder et al. (2011) successfully investigated intracellular water in different plant-based food tissues using BIA and found 78–96% water present in intracellular space. Due to the limitations of the method (discussed below), it may not possible to detect the proportion of SBW (cell wall water) in plant-based food tissue. Therefore, this method can be recommended for the researcher who would like to investigate free and LBW in different biological tissues.**

2.2.4 Limitations of BIA

BIA is popular for analyzing tissue composition because it is noninvasive, and it is less time consuming and simpler than other methods. BIA is mainly used for analyzing the proportion of fat in animal tissue (Dean et al., 2008; Webber & Dehnel, 1968), particularly for human tissue. Although many have researchers used BIA for postharvest quality assurance purposes (Cox et al., 1993; Dejmek & Miyawaki, 2002; Zhang MIN, 1990). **For any technique, calibration is important before starting the experiment. However, calibration procedure required in BIA is complex, which limits BIA's utility for plant tissue analysis (Dehghan & Merchant, 2008). Moreover, many factors affect the validity of the method. For instance, tissue geometry strongly affects the result, which ultimately affects the validity of the method (Deurenberg, 1996). Therefore, calibration should be done properly before this method can be used for investigating water status in diverse biological tissue.**

2.3 Dilatometry (DIL)

2.3.1 Theory

Dilatometry is a **thermo-**analytical technique that can be used for measuring bound water, based on thermal expansion or contraction of material while subjected to a controlled temperature. This method takes advantage of the fact that when water freezes it expands about 9% in volume. In this procedure, the sample and a nonfreezing (at the temperatures employed) indicator fluid are entered into the dilatometer as shown in Figure 7. The change in the level of the meniscus of the indicator fluid indicates the change in volume of the freezing sample. Moreover, if a sample of material of known water content is immersed in a liquid with a low freezing point and that is immiscible with water and enclosed in a system in which small changes in volume can be measured, the expansion accompanying freezing can be measured, and the amount of water that froze can be calculated. Then from this amount, the amount of unfrozen or bound water can be calculated.

During dilatometry measurements, it can be assumed that the bound portion of water is held by forces greater than those which act to orient water molecules into the crystal lattice of ice.

[Figure 7 can be inserted here]

The main mechanism of dilatometry is the thermal expansion or contraction of material. The thermal expansion or contraction can be calculated from the following equation:

$$\frac{\Delta V}{V} = \exp\left(\int_{1}^{T_2} \alpha_V(T)dT\right) - 1 \qquad (11)$$

where V is the volume of the material (m^3), T_1 and T_2 are the initial and final temperatures, and α_V is the volumetric thermal expansion coefficient as a function of temperature.

For anisotropic fruit structures, thermal expansion coefficients may be different in different directions (x, y, and z). Consequently, the total volumetric expansion is distributed unequally along the three axes. In such cases, it is necessary to treat the coefficient of thermal expansion as a tensor with up to six independent elements. Thermal expansion generally decreases with increasing bond energy, and volumetric expansion or contraction changes the thermal expansion coefficient. Therefore, the bound water, which has strong bonding energy with a solid, can be readily found.

2.3.2 Working procedure of dilatometry

For the dilatometry measurement, the prepared sample should be placed into the sample holder (usually referred to as the dilatometer tube). The position of the sample holder may be horizontal or vertical. The sample should be in contact with the pushrod to transmit the signal to the displacement sensor (or transducer). It is necessary to check that the sample is in contact with the pushrod throughout the process. When the sample expands or contracts, it pushes or pulls the tube and the pushrod in opposite directions. This movement is detected by the displacement sensor. From the transducer signal, an expansion (heating) or a contraction (cooling) curve can be found. From this curve, an expansion or contraction coefficient can be measured. The FW can be calculated using the following equation.

$$FW = \frac{D + (W \times A \times \Delta T)}{\xi} \tag{12}$$

where D is the level difference in the dilatometer from ΔT, W is the weight of the reference material, A is the concentration coefficient of reference material, ΔT is the temperature

difference, and ξ is the expansion or contraction coefficient that can be found from the expansion or contraction curve (Wu, Huang, & Lee, 1998).After calculating the FW, bound water can be calculated by subtracting FW from the total water content.

2.3.3 Current status of dilatometry application in biological tissue analysis

This method is a very popular technique for the researcher who investigates the bound water in sludge and soil (Lee, 1996; Smith & Vesilind, 1995; Wu et al., 1998), and polymers (Tatauko Hatakeyama et al., 1988). However, it has seldom been used for the investigation of bound water in plant-based food tissue. This is may be because of some limitations of this technique discussed below.

2.3.4 Limitations of Dilatometry

During dilatometry analysis, it is necessary to ensure that all the air is removed from the material before the readings are taken (Sayre, 1932) because this method is prone to artifacts caused by trapped air (Steele, 2004). Most plant-based food materials are hygroscopic in nature and thus it contains air and vapor in intercellular spaces. Therefore, dilatometry may be not suitable for investigation of bound water in plant-based food material (Khan et al., 2016b). Thus, this method is best suited for investigation of bound water in non-hygroscopic materials such as soil, wastewater, and sludge. **There are some food materials which have characteristics very close to non-hygroscopic materials. Researcher may try to use this method in investigating such food materials.**

2.4 Thermogravimetric Analysis (TGA)

2.4.1 Theory

Thermogravimetric Analysis (TGA) is a technique in which the mass of a substance is scrutinised as a function of temperature with the constant heating rate or time as the sample is subjected to a controlled temperature program in a controlled atmosphere. In TGA, the sample is usually heated at a constant heating rate, which sometimes is called as dynamic measurement process. Moreover, it can also be possible to conduct TGA at a constant temperature (e.g. isothermal process), although it may be subjected to non-linear temperature programs like those used in controlled TGA (so-called SCTA) experiments (Bottom, 2008). The choice of temperature program will depend upon the type of information required for the sample. It is very important to ensure a controlled environment (e.g. inert or reactive) for the TG analysis in order to minimise oxidation or other undesired reactions. A TGA consists of a sample pan that is supported by a precision balance. The pan is located in an oven, and is heated or cooled during the experiment. The weight of the sample should be monitored continuously and precisely during the experiment. The results of a TGA measurement are usually displayed as a TGA curve in which mass or percentage of weight is plotted against temperature or time, as shown in Figure 8. A first derivative of the plotted TGA curve can provide the rate at which the mass changes and is known as the differential thermogravimetric or DTG curve (Figure 8). Moreover, a point of inflection is found from the DTG curve which can provide the in-depth interpretations of water status in different biological tissues.

[Figure 8 can be inserted here]

2.4.2 Working procedure of Thermogravimetric analysis

For the TGA experiments, the sample should be prepared with proper care and the size of the sample should be accurate. The size of the sample depends on the diverse nature of the biological tissues. It is preferred that the sample weight should be between 2 to 50 mg [ref]. It is expected that the all the samples used in an investigation should have same weight to ensure the best results and reproducibility of findings. Moreover, many small pieces of sample should be used instead of one large chunk as large samples provide a greater surface area exposed to the sample purge. TG analyser usually consists of a high-precision microbalance with a pan (generally platinum) that is located in a small electrically heated oven with a thermocouple to measure the temperature accurately. The prepared samples then should be loaded in the pan and continuously heated at a specific temperature (usually room temperature to 1000^{0}C) at a constant heating rate. As the temperature increases, various components of the sample are changed due to the heterogeneous chemical reaction. Moreover, while increasing the temperature, the weight of the samples decreases. This is because of the moisture loss of the sample through evaporation. The TGA analyser continuously records the change of temperature with the change of sample weight and stored it for the further analysis.

For the data analysis, the temperature should be plotted on the X-axis and mass loss on the Y-axis. Then the data can be adjusted using curve smoothing. The first derivatives are often plotted to determine points of inflection for further in-depth interpretations. The weight loss at different temperatures can be interpreted from the TGA curve. It is considered that free water is evaporated quickly at a specific temperature, and the remaining water is the bound water. A general trend of TG curve and DTG curve was drawn for the interpretation of free and bound water as shown in

Figure 8. From this figure, it can be seen that free water decreased steadily up to specific moisture content while bound water remains stable up to a specific temperature. This is may be due to the fact that micromolecular bonding strength of bound water does not allow migration of bound water at the early stage of heating. Further details can be found the literature (Biscarat, Charmette, Sanchez, & Pochat-Bohatier, 2015; Bottom, 2008). These studies provide a detail experimental procedure of TG analysis.

2.4.3 Current status of TG application in biological tissue analysis

The TG is a well-known technique that is widely used for chemical deposition, combustion analysis, material decomposition analysis, and soil analysis including some biological tissue analysis (Coats & Redfern, 1963). It has been reported that thermogravimetric analysis is successfully used in determining hygroscopic moisture, organic matter, and inorganic carbonates in soil (Kristl, Muršec, Šuštar, & Kristl, 2016; Miyazawa, Pavan, De Oliveira, Ionashiro, & Silva, 2000; Pallasser, Minasny, & McBratney, 2013). Chan, Murthi, and Harrison (1970) have used the thermogravimetry for investigating the calcium and magnesium in dolomite rock. Berlin and Robinson have used thermogravimetry in their determination of magnesium, potassium and lead with dilituric acid, and for determining ethylenediamine and quinine with the same precipitant (Berlin & Robinson, 1961). Due to diverse nature of biological tissue, the application of TG is relatively rare in this area. Feng, Tang, and John Dixon-Warren (2000) successfully used TG for investigating the moisture diffusivity in apple tissues. Silva, Silva, Andrade, Veloso, and Santos (2008) investigated the water activity and moisture distribution in algae and fish using this technique. They suggested that TG is the suitable technique that can be used to determine moisture content in biological samples. Biscarat, Charmette, Sanchez, and Pochat-Bohatier (2015) identified free and bound water in gelatin membrane using TG method. However, they did not determine the proportion of LBW

and SBW in gelatin membrane. This may be due to the limitations of the method. Although this technique has some limitations (discussed below), it could be one of the options for investigating the free and bound water distribution while drying is in progress as this methods measures the water proportion with continuous temperature increase.

2.4.4 Limitations of Thermogravimetric analysis

Although this method is useful for determining free and bound moisture distribution, some limitations of this approach make it difficult to obtain accurate results. For example, it is very difficult to obtain the plateau at one particular heating rate in complex materials like food. Therefore, insufficient and inaccurate data may be obtained due to the lack of appearance of the plateau at a specific heating rate. Moreover, data interpretation of the TG method is not always straightforward. For better interpretation, the TGA analysis is usually done in combination with other techniques. In TG analysis, sample size is restricted between 2-50mg, which significantly limits the suitability of some investigations. For example, for investigating water distribution during drying, the sample will quickly reach dried condition and an error may appear due to the sensitivity to small mass loss effects.

2.5 Nuclear magnetic resonance (NMR)

2.5.1 Theory

NMR is a uniquely effective tool to trace the cellular water environment and analyze the quality parameters. It is an established technique for examining the chemical environment of atomic nuclei with an odd number of protons and/or neutrons. Such nuclei have a magnetic moment that processes in a magnetic field with a characteristic frequency, known as the Larmor

frequency. When placed in the presence of a strong magnetic field, a (small) proportion of the nuclei align with the magnetic field in an antiparallel manner similar to a bar-magnet in a magnetic field. The number of spins aligning in this manner is proportional to the strength of the magnetic field, with the end result being a sample with a net magnetization vector that can be studied spectroscopically. The distribution of nuclei between the ground state and the aligned, lower energy state is given by the Boltzmann relation (Abragam, 1961; Hanson, 2008).

$$\frac{N_{upper}}{N_{lower}} = e^{-\Delta E/kT} = e^{-h\nu/kT} \qquad (13)$$

where the difference in energy of the two states is ΔE, k is the Boltzmann constant, T is the absolute temperature, h is Planck's constant, and ν is the resonant frequency. For a magnetic field strength of 18.8 tesla (800 MHz for protons), at thermal equilibrium and at room temperature, the ratio of nuclei in the two energy states is 0.999872. This small population difference is utilized by the NMR technique and is the source of the technique's low sensitivity.

Nuclei with a magnetic moment have a specific gyromagnetic ratio γ and the resonant frequency ν_o is dependent on the magnetic field strength B_o (Derome, 2013) such that

$$\nu_o = \frac{\gamma B_o}{2\pi} \qquad (14).$$

Application of a short radio frequency signal matched to the precession frequency of the nucleus of interest results in absorption of energy and coherent precession of the nuclei. The net magnetization vector is moved out of alignment with the magnetic field. The degree of rotation of the magnetization vector is determined by the power of the radio frequency pulse. When the radio frequency signal ceases, the nuclei return to the equilibrium state and their spins lose coherence.

The NMR signal is measured after application of the radio frequency pulse by placing the sample in a coil that is tuned to the resonance frequency of the nuclei of interest. The coherently processing magnetic moment of the nuclei induces a small current in a receiver coil,

which decays as the nuclei return to equilibrium. The resulting intensity–time signal can be recorded and is Fourier transformed to yield an intensity–frequency spectrum. The maximum magnetization that can be detected M_o is given by

$$M_o = \frac{\gamma^2 h^2 N_s B_o}{4kT} \qquad (15).$$

where γ is the nuclear species-specific gyromagnetic ratio, N_s is the number of spins, and B_o is the magnetic field strength (Hanson, 2008). It can be seen from this equation that the strength of the recorded signal is proportional to the number of nuclei in the sample volume and the strength of the applied magnetic field. In the presence of a strong external magnetic field, the local magnetic field experienced by a nucleus is influenced by the electrons in its immediate environment. Thus, the molecular structure in which an atom participates can alter the precise resonant frequency of the nucleus. This behavior in the presence of different electronic environments results in populations of spins corresponding to the electron-shielding experienced by nuclei in each environment. This information is utilized to generate an NMR spectrum, and the signal dispersion due to local shielding effects is termed chemical shift.

The return to alignment with the magnetic field is described by a relaxation time constant T_1 (spin–lattice relaxation), and the loss of coherence is described by a relaxation time constant T_2 (spin–spin relaxation). When nuclei are in a restricted environment, energy is lost to the surrounding atoms (lattice) and T_1 is shortened, relative to an equivalent nucleus in a less constrained environment. T_2 relaxation results from interaction between the processing spins of the excited nuclei. This form of relaxation can be equal to or shorter than T_1 relaxation, depending on local environments of the nuclei (Derome, 2013). An advantage arising from the change in relaxation time constants with environment is the ability to relate the relaxation time to the mobility of the nuclei being studied, with longer relaxation times being associated with

more mobile nuclei. Conversely, nuclei that are in a restricted environment will have a shorter relaxation time.

The NMR signal can be spatially localized by making use of the frequency's dependence on magnetic field strength. Application of a linear magnetic field gradient across a sample can be achieved by passing a current through "gradient" coils that are integrated within the static magnetic field of the NMR magnet. The resulting distortion of the B_o magnetic field by the current applied to the gradient coils provides a gradation of the magnetic field that results in a distribution of resonance frequency for a population of nuclei, based on their spatial position within the sample (in the direction of the applied gradient). Stepwise variation in the strength of the current enables a corresponding localization of nuclei across the sample. Spatial information in a second dimension is obtained by using phase encoding of the applied radio frequency signal. The slice thickness of the two-dimensional plane created by the imaging sequence is controlled by the application of an orthogonal gradient and radio frequency pulse. The image resulting from a Fourier transformation of the acquired data provides a map of the signal intensity throughout the plane of interest. The stepwise technique results in the measurement of signals from discrete regions or voxels. This spatial encoding of the NMR signal forms the basis of magnetic resonance imaging (MRI). Because the signal is proportional to the number of nuclei in each voxel, the reduced size of the effective sample results in a smaller signal. For this reason, only nuclei with the greatest NMR sensitivity (i.e., the largest gyromagnetic ratio), such as ^{1}H, are suitable for MRI. In biological systems, tissue water provides the greatest concentration of ^{1}H nuclei and therefore the strongest signal in biological samples.

Examining the signal from water in biological samples forms the basis of most MRI studies. The information recorded can range from distribution mapping of the concentration of water to the spatial mapping of relaxation times as a marker of differences in the local

environment or tissue water. By selecting imaging sequence timing parameters, the regional intensity of concentration-based images can be filtered according to the relaxation parameters that are influenced by the tissue environment.

2.5.2 Working procedure during NMR experimentation

Proton NMR (^{1}H-NMR) relaxometry studies have proven to be valuable in the study of plants and plant-based food materials subjected to stress, reflecting anatomical details of the entire tissue and the water status in particular (Gambhir, Choi, Slaughter, Thompson, & McCarthy, 2005; L. Van Der Weerd et al., 2002). ^{1}H-NMR relaxometry signals, which are an average over the whole sample, provide information on the water environments within the plant tissue since, as described above, the proton signal is dominated by water protons (Louise van der Weerd et al., 2001) and the proton NMR signal intensity is directly proportional to the proton density of the tissue (Westbrook & Roth, 2011). The water exchange rates between these compartments are controlled by the water proton relaxation behavior T_2 that strongly depends on the water mobility in the microscopic environment of the tissue and the strength of the applied magnetic field. The spin–spin T_2 relaxation is the transverse component of the magnetization vector, which exponentially decays toward its equilibrium value after excitation by radio frequency energy. It can be expressed as

$$M(t) = \sum_{i=1}^{n} A_i \, e^{-t/T_2^i} \qquad (16).$$

where $M(t)$ is the function of relaxation time, A is the relative contribution of sets of protons, T_2 is the relaxation time of water proton, and i is the number of the contributing components.

To decide whether the T_2 signal contains one or more components, the T_2 signal can be fitted with a mono-exponential model. Fitting a mono-exponential function will result in an erroneous value for T_2 if more than one component is present. In such cases, we need to fit for the additional component(s). The number can be estimated by plotting the natural logarithm of the signal $M(t)$ against time, after which it can be straight forward to see if the function is bi-exponential or tri-exponential, as there will be distinct linear regions of differing slope in the resulting plot (Boulby & Rugg–Gunn, 2004). However, for optimum accuracy, this model requires a good signal-to-noise ratio (SNR). **The signal-to-noise ratio measurement is an important criterion for accurate integrations, and is also one of the best ways to determine the sensitivity of a NMR spectrometer. In general, a higher SNR specification means that the instrument is more sensitive. For any sample, an optimum SNR is achieved using a line broadening equal to the peak width at half height. The following equation is used for calculating SNR.**

$$SNR = \frac{2.5H}{N_{pp}} \qquad \textbf{(17).}$$

Where, H is the height of the chosen peak, and N_{pp} is the peak-to-peak noise.

If SNR is low, the fit to the four parameters (A_1, A_2, T_{21}, T_{22}) for the bi-exponential model or six parameters (A_1, A_2, A_3, T_{21}, T_{22}, T_{23}) for the tri-exponential model becomes uncertain, reducing accuracy and precision. In addition, the relaxation times should be within the same order of magnitude (and preferably should differ by no more than a factor of 2–3), and the population fractions ideally should not fall below about 15%. Sometimes it is possible that even more components may be present. In such cases the best approach is to use a statistical test to determine whether or not additional terms need to be added to the fit (Armspach, Gounot, Rumbach, & Chambron, 1991).

To deduce free and bound water from T_2^i signal intensity, the relative contribution A_i can be categorized according to the pore size, water content, membrane permeability, and the proton density within the sample (Boulby & Rugg–Gunn, 2004; Khan et al., 2016b). Moreover, water mobility at the molecular level influences T_2 relaxation. The water mobility is defined as the ability of water molecules to rotate freely as well as moving spatially, with the result that T_2 is inversely proportional to rotational motion (which is a reflection of inherent mobility) (Nelson, 2003). It has been reported that water in a restrictive environment shows short relaxation times (Boulby & Rugg–Gunn, 2004; Wheeler-Kingshott, Barker, Steens, & van Buchem, 2004), and T_2 is also short when water is strongly interacting with macromolecules (Rondeau M.C., 2014). In plant-based food material, the cell wall is mostly composed of solid matter with very low water content. This structure acts to restrict translational motion and increase the correlation time of water (Boulby & Rugg–Gunn, 2004). Therefore, the short T_2 component is most likely to relate to cell wall water (SBW). Furthermore, it has been stated that the majority of water is present in intracellular spaces that act as a water reservoir with a predominantly water–water interface (Joardder, Kumar, & Karim, 2017; Khan et al., 2016a; Khan et al., 2016b; PS., 2009) where the water protons relax slowly (Berna, 2010), resulting in a longer T_2 relaxation. Among the many T_2 components fitted, the longest component had the greater water fraction. Based on the water content of the sample, it can be related to the intracellular water (LBW) (Khan et al., 2016). The remaining component (medium) then relates to the FW.

2.5.3 Current status of NMR application in biological tissue analysis

In biological science, NMR spectroscopy is one of the most powerful analytical techniques for investigating biological tissue composition. Recently, NMR has been used to show water compartmentation in a number of animal tissues: lung (Cutillo, Morris, Ailion,

Durney, & Ganesan, 1992; Sedin et al., 2000), brain (Berenyi, Repa, Bogner, Doczi, & Sulyok, 1998; Furuse et al., 1984; Inao et al., 1985; Sulyok et al., 2001; Vajda et al., 1999), liver (Moser, Holzmueller, & Gomiscek, 1992; Moser, Holzmueller, & Krssak), and red blood cells (Besson, Wheatley, Skinner, & Foster, 1989). In the case of plant-based food material, T_2 relaxation theories have been applied to the investigation of sugar content in fruit tissue (Delgado-Goni et al., 2013), the quality of fruits and vegetables (Chen, 1989; Van de Velde, Grace, Esposito, Pirovani, & Lila, 2016), and the maturity of fruits and vegetables (Chen, McCarthy, Kauten, Sarig, & Han, 1993; Ruan, Chen, & Almaer, 1999); however, literature describing the measurement of free and bound water in plant-based food materials is rare. Hills and Remigereau (1997) investigated T_2 relaxation times for assessing the migration of different types of water during drying and freezing in apple tissue, but they did not quantify the types of water in that tissue. Gonzalez et al. (2010) studied the effect of high pressure on cell membrane integrity during thermal processing of onion. But while they investigated the change in T_2 with processing time, they did not report data on the proportion of FW, LBW, and SBW in the onion tissue. Previous NMR experiments have used T_2 relaxometry to study postharvest changes for quality assurance purposes. Studies have been conducted on the development of the water core (Cho et al., 2008; Clark et al., 1998; Melado-Herreros et al., 2013), internal browning (Cho et al., 2008; Clark & Burmeister, 1999; Gonzalez et al., 2001) and microstructural heterogeneity (Defraeye et al., 2013; Winisdorffer et al., 2015) in apple tissue; but the proportions of FW, LBW, and SBW have gone unreported.

Very recently, Khan et al. (2016b) investigated FW, LBW, and SBW for different plant-based food materials. They argued that depending on the food structure and physical characteristics, about 80–90% LBW, 2–5% SBW, and 10–20% FW are present in different fruit materials. However, Khan et al. (2016b) did not show the effect of maturity on cellular

water distribution in plant-based food material. The distribution of cellular water depends on the maturity of fruits and vegetables.

2.5.4 Limitations of NMR application in biological tissue

To investigate the different cellular compartments of water, NMR can be considered a unique tool, but it has some limitations. The disadvantages of NMR predominantly relate to the low sensitivity of the technique. Due to the low number of nuclei aligned with the magnetic field, significant signal averaging is required to obtain a satisfactory SNR. Measurement of water in biological systems provides a reasonable signal but when molecules other than water are examined, this low sensitivity becomes a greater problem. The measurement of nuclei other than protons amplifies the problem of low SNR because of their lower gyromagnetic ratio. Measurement of such samples requires either high concentrations of the measured nuclei, or longer acquisition times, or a combination of both.

NMR measurement is not possible for nuclei that do not have a magnetic moment and even for those that are NMR sensitive, because the technique relies on an environment with a homogeneous magnetic field. At the molecular level this can be disrupted by paramagnetic nuclei, which reduce the NMR sensitivity. The strong superconducting magnets used in NMR systems are associated with significant costs, being expensive and requiring regular maintenance of cryogen levels.

Despite these disadvantages, the wealth of information available from NMR experiments makes the technique extremely valuable.

3. Cellular water distribution in plant-based food tissue: current status

There are three major cellular environments containing water in plant-based food material. Different cellular environments contain different proportions of water. It has been

found that the majority of water (80–96%) in food tissue is present in the intracellular environment, only 8–15% water is present in intercellular spaces, and a smaller amount of water (6–4%) exists in the cell wall environment (Khan et al., 2016b). This proportion of cellular water depends on its structure and properties. Due to the structural heterogeneity and diversity of food, different types of food materials contain different amounts of FW, LBW, and SBW. Khan et al. (2016b) investigated the proportions of cellular water in five different fruits (apple, kiwi, pear, nectarine, and apricot) and six different vegetables (potato, carrot, pumpkin, cucumber, tomato, and eggplant) **using ^{1}H-NMR T_2 relaxometry. The T_2 relaxation decay curves were obtained from samples at different drying times. Each curve was then fitted using the multi-exponential decay equation (16). After fitting the Tri-exponential decay curve with different T_2 relaxation intensity data, three different proton components of water relaxation (long, medium, and short) were determined. Depending on the water mobility and pore size, three signal components were categorized as LBW, FW, and SBW.** They found that, of the fruits, apple contained the highest proportion of LBW (about 90%), while kiwi fruit demonstrated the least amount of LBW (about 80%). On the other hand, of the six vegetables, eggplant contained the greatest amount of LBW (about 92%), followed by cucumber and tomato. Halder et al. (2011) investigated intracellular water in different plant-based food materials using the BIA method. They confirmed that about 78–96% water was present in the intracellular environment, depending on the types of fruit and vegetable. However, they did not investigate the proportion of FW and SBW present in plant-based food material. The water distribution discussed above was measured in fresh food samples. Measurements dealing with the cellular water distribution during drying have not been made because the mechanisms of cellular water transport are unclear. Table 1 shows a list of food materials with their proportion of FW, LBW, and SBW as measured in the two studies discussed.

[Table 1 can be inserted here]

4. Challenges to determining cellular water

4.1 Finding cellular level water distribution

Accurate understanding of different cellular level of water is important for interpreting actual heat and mass transfer during drying (Khan et al., 2016a). To the best of our knowledge, there is only one study that deals about the percentage of FW, SBW, and LBW (Khan et al., 2016b) in different fresh food samples. This study investigated the percentage of FW, LBW, and SBW in various food materials using NMR T_2 relaxometry. As discussed above, NMR sometimes provides inaccurate data due to its sensitivity problem; therefore, a single study (Khan et al., 2016b) is insufficient to generate a realistic understanding of the different cellular water investigation in plant-based food material. To find actual FW, SBW, and LBW in fresh food samples remains a further challenge for future research.

Furthermore, to understand the transport mechanism of water at the cellular level during drying, it is crucial to investigate how the water moves from one cellular environment to other while drying is in progress. However, to the authors' knowledge there is no published study that has investigated how cellular water moves from the intracellular environment to the intercellular environment. Therefore, it is a major challenge for food drying researchers to discover the cellular level water transport mechanism during drying.

4.1 Selecting the appropriate method

There are many methods to investigate bound water; however, the only method suitable to investigate cellular level water in plant-based food is NMR. Although NMR is a uniquely

useful tool for tracing cellular level water, poor sensitivity and resulting noisy data are significant issues. The main challenge to analyzing NMR data is the sensitivity of the analysis. During NMR experimentation, most of the data collected is noisy and therefore the SNR deteriorates (Wheeler-Kingshott et al., 2004). A poor SNR can result in erroneous interpretation of the data concerning SBW, LBW, and FW. Therefore, producing noise-free data with better sensitivity is the ultimate challenge to the investigation of cellular level water distribution using NMR.

4.2 Properties and parameters required

The accuracy of a mechanistic model considering bound water transport depends on the availability of appropriate transport **properties of food material** (Khan et al., 2016a). Intracellular water diffusivity, thermal conductivity, permeability, and capillary pressure are the most significant properties of plant-based food materials that need to be considered while considering transport of bound water during drying. Due to the lack of data regarding these thermal properties, researchers use their estimated values in complex models, which can lead to large errors in final solutions (Feng et al., 2001). Real-time measurement of these properties is very difficult and this is the main reason for the scarcity of data. Therefore, measurement of these properties, along with real-time heat and mass transfer, demands special attention.

5. Conclusion

In this article, a comprehensive review of cellular level water types and investigation techniques have been presented. Differentiating between types of bound water according to bonding strength and cellular environment has been discussed. This review has also evaluated the consideration of bound water transport in existing food processing models and cellular

water investigation techniques (NMR, DSC, BIA, and dilatometry) have been discussed. It was found that NMR can be considered the most efficient technique for measuring the different types of cellular water in plant-based food material. Also discussed were the current challenges to investigating cellular water in fresh food samples and moisture migration mechanisms during drying. This review article contributes to a better understanding of cellular water distributions, its transport mechanisms, and investigation methods for food researchers.

Acknowledgment

The authors are sincerely grateful to the Queensland University of Technology, Australia for funding a QUTPRA scholarship and HDR Tuition Fee Sponsorship, which has enabled the conduct of this research.

References

Abbott, J. A., Renfu, Lu., Upchurch, B. L., & Stroshine, R. L. (2010). Technologies for Nondestructive
Quality Evaluation of Fruits and Vegetables. *Horticultural Reviews, 20, 1-120.*

Abragam, A. (1961). *The principles of nuclear magnetism*: Oxford university press.

Aguilera, J. M., & Stanley, D. W. (1999). Simultaneous heat and mass transfer: dehydration. Microstructural Principles of Food Processing and Engineering, 2nd edn. Aspen Publishers, Inc, Gaithersburg.

Aktaş, N., Tülek, Y., & Gökalp, H. Y. (1997). Determination of differences in free and bound water contents of beef muscle by DSC under various freezing conditions. *Journal of thermal analysis, 50*(4), 617-624. doi:10.1007/bf01979033

Alejandro, G., Marangoni, M.F.P.(2014). Differential Scanning Calorimetry, AOCS Lipid library

Armspach, J.P., Gounot, D., Rumbach, L., & Chambron, J. (1991). In vivo determination of multiexponential T_2 relaxation in the brain of patients with multiple sclerosis. *Magnetic Resonance Imaging, 9*(1), 107-113.

Berenyi, E., Repa, I., Bogner, P., Doczi, T., & Sulyok, E. (1998). Water content and proton magnetic resonance relaxation times of the brain in newborn rabbits. *Pediatr Res, 43*(3), 421-425. doi:10.1203/00006450-199803000-00019

Berna, F. (2010). Scientific Methods and Cultural Heritage. An Introduction to the Application of Materials Science to Archaeometry and Conservation Science, ed Artioli G: Oxford Univ Press, Oxford.

Besson, J. A., Wheatley, D. N., Skinner, E. R., & Foster, M. A. (1989). 1H-NMR relaxation times and water content of red blood cells from chronic alcoholic patients during withdrawal. *Magn Reson Imaging, 7*(3), 289-291.

Boulby, P. A., & Rugg–Gunn, F. J. (2004). T2: The Transverse Relaxation Time. *Quantitative MRI of the Brain* (pp. 143-201): John Wiley & Sons, Ltd.

Bramhall, G. (1979). Sorption diffusion in wood. *Wood science, 12*, 3-13.

Briggs, D. R. (1932). Water relationships in colloids. II. *The Journal of Physical Chemistry, 36*(1), 367-386.

Berlin, A., & Robinson, R. J. (1961). Thermogravimetric determination of magnesium, potassium and lead by precipitation with dilituric acid. *Analytica Chimica Acta, 24*, 224-234.

Biscarat, J., Charmette, C., Sanchez, J., & Pochat-Bohatier, C. (2015). Preparation of dense gelatin membranes by combining temperature induced gelation and dry-casting. Journal of Membrane Science, 473, 45-53. doi:https://doi.org/10.1016/j.memsci.2014.09.004

Bottom, R. (2008). Thermogravimetric Analysis Principles and Applications of Thermal Analysis (pp. 87-118): Blackwell Publishing Ltd.

Caurie, M. (2011). Bound water: its definition, estimation and characteristics. *International Journal of Food Science & Technology, 46*(5), 930-934. doi:10.1111/j.1365-2621.2011.02581.x

Chen, P., McCarthy, M. J., Kauten, R., Sarig, Y., & Han, S. (1993). Maturity Evaluation of Avocados by NMR Methods. *Journal of Agricultural Engineering Research, 55*(3), 177-187. doi:http://dx.doi.org/10.1006/jaer.1993.1042

Cho, B. K., Chayaprasert, W., & Stroshine, R. L. (2008). Effects of internal browning and watercore on low field (5.4 MHz) proton magnetic resonance measurements of T2 values of whole apples. *Postharvest Biology and Technology, 47*(1), 81-89. doi:http://dx.doi.org/10.1016/j.postharvbio.2007.05.018

Clark, C. J., & Burmeister, D. M. (1999). Magnetic resonance imaging of browning development in 'Braeburn' apple during controlled-atmosphere storage under high CO2. *Hort Science, 34*(5), 915-919.

Clark, C. J., MacFall, J. S., & Bieleski, R. L. (1998). Loss of watercore from `Fuji' apple observed by magnetic resonance imaging. *Scientia Horticulturae, 73*(4), 213-227. doi:http://dx.doi.org/10.1016/S0304-4238(98)00076-4

Chen, P., McCarthy, M. J., & Kauten, R. (1989). NMR for internal quality evaluation of fruits and vegetables. Trans. ASAE, 32(5), 1747-1753.

Cox, M. A., Zhang, M. I. N., & Willison, J. H. M. (1993). Apple bruise assessment through electrical impedance measurements. *Journal of Horticultural Science, 68*(3), 393-398. doi:10.1080/00221589.1993.11516366

Cutillo, A. G., Morris, A. H., Ailion, D. C., Durney, C. H., & Ganesan, K. (1992). Determination of Lung Water Content and Distribution by Nuclear Magnetic Resonance. In E. Rügheimer (Ed.), *New Aspects on Respiratory Failure* (pp. 138-146). Berlin, Heidelberg: Springer Berlin Heidelberg.

Chan, R., Murthi, K., & Harrison, D. (1970). Thermogravimetric analysis of Ontario limestones and dolomites I. Calcination, surface area, and porosity. *Canadian Journal of Chemistry, 48*(19), 2972-2978.

Coats, A., & Redfern, J. (1963). Thermogravimetric analysis. A review. Analyst, 88(1053), 906-924.

Datta, A. K. (2007). Porous media approaches to studying simultaneous heat and mass transfer in food processes. I: Problem formulations. *Journal of Food Engineering, 80*(1), 80-95. doi:http://dx.doi.org/10.1016/j.jfoodeng.2006.05.013

Dean, D. A., Ramanathan, T., Machado, D., & Sundararajan, R. (2008). Electrical impedance spectroscopy study of biological tissues. *Journal of Electrostatics, 66*(3–4), 165-177. doi:http://dx.doi.org/10.1016/j.elstat.2007.11.005

Defraeye, T., Lehmann, V., Gross, D., Holat, C., Herremans, E., Verboven, P., Verlinden, B. E., & Nicolai, B. M. (2013). Application of MRI for tissue characterisation of 'Braeburn' apple. *Postharvest Biology and Technology, 75*, 96-105. doi:http://dx.doi.org/10.1016/j.postharvbio.2012.08.009

Dehghan, M., & Merchant, A. T. (2008). Is bioelectrical impedance accurate for use in large epidemiological studies? *Nutrition Journal, 7*, 26-26. doi:10.1186/1475-2891-7-26

Dejmek, P., & Miyawaki, O. (2002). Relationship between the electrical and rheological properties of potato tuber tissue after various forms of processing. *Biosci Biotechnol Biochem, 66*(6), 1218-1223. doi:10.1271/bbb.66.1218

Delgado-Goni, T., Campo, S., Martin-Sitjar, J., Cabanas, M. E., San Segundo, B., & Arus, C. (2013). Assessment of a ^{1}H high-resolution magic angle spinning NMR spectroscopy procedure for free sugars quantification in intact plant tissue. *Planta, 238*(2), 397-413. doi:10.1007/s00425-013-1924-y

Derome, A. E. (2013). *Modern NMR techniques for chemistry research*: Elsevier.

Deurenberg, P. (1996). Limitations of the bioelectrical impedance method for the assessment of body fat in severe obesity. *Am J Clin Nutr, 64*(3 Suppl), 449s-452s.

De Lorenzo, A., Andreoli, A., Matthie, J., & Withers, P. (1997). Predicting body cell mass with bioimpedance by using theoretical methods: a technological review. Journal of Applied Physiology, 82(5), 1542-1558.

Diao, J., Zhou, Z., Li, N., Nie, H., Yu, H., & Xu, H. (2012). High accuracy biological impedance measurement system design and calibration. In Digital Manufacturing and Automation (ICDMA), 2012 Third International Conference on (pp. 466-470). IEEE.

Dart, J. A. & Newman, D. S. M. (2005). Watercore of Apples. NSW Department of Primary Industries, PRIMEFACT-49, Australia.

Feng, H., Tang, J., & John Dixon-Warren, S. (2000). Determination of moisture diffusivity of red delicious apple tissues by thermogravimetric analysis. *Drying Technology, 18*(6), 1183-1199.

Feng, H., Tang, J., Cavalieri, R., & Plumb, O. (2001). Heat and mass transport in microwave drying of porous materials in a spouted bed. *AIChE Journal, 47*(7), 1499-1512.

Furuse, M., Gonda, T., Kuchiwaki, H., Hirai, N., Inao, S., & Kageyama, N. (1984). Thermal Analysis on the State of Free and Bound Water in Normal and Edematous Brains. In K. G. Go & A. Baethmann (Eds.), *Recent Progress in the Study and Therapy of Brain Edema* (pp. 293-298). Boston, MA: Springer US.

Gambhir, P. N., Choi, Y. J., Slaughter, D. C., Thompson, J. F., & McCarthy, M. J. (2005). Proton spin–spin relaxation time of peel and flesh of navel orange varieties exposed to freezing temperature. *Journal of the Science of Food and Agriculture, 85*(14), 2482-2486. doi:10.1002/jsfa.2266

Gill, P., Moghadam, T. T., & Ranjbar, B. (2010). Differential Scanning Calorimetry Techniques: Applications in Biology and Nanoscience. *Journal of Biomolecular Techniques: JBT, 21*(4), 167-193.

Goñi, O., Fernandez-Caballero, C., Sanchez-Ballesta, M. T., Escribano, M. I., & Merodio, C. (2011). Water status and quality improvement in high-CO2 treated table grapes. *Food Chemistry, 128*(1), 34-39. doi:http://dx.doi.org/10.1016/j.foodchem.2011.02.073

Gonzalez, J. J., Valle, R. C., Bobroff, S., Biasi, W. V., Mitcham, E. J., & McCarthy, M. J. (2001). Detection and monitoring of internal browning development in 'Fuji' apples using MRI. *Postharvest Biology and Technology, 22*(2), 179-188. doi:http://dx.doi.org/10.1016/S0925-5214(00)00183-6

Gonzalez, M. E., Barrett, D. M., McCarthy, M. J., Vergeldt, F. J., Gerkema, E., Matser, A. M., & Van As, H. (2010). ^{1}H-NMR study of the impact of high pressure and thermal processing on cell membrane integrity of onions. *J Food Sci, 75*(7), 417-425. doi:10.1111/j.1750-3841.2010.01766.x

Grimnes, S. and Martinsen O. G. (2007). Sources of error in tetrapo lar impedance measurements on biomaterials and other ionic conductors. J. Phys. D: Appl. Phys., 40, 9-14.

Haines, P., Reading, M., & Wilburn, F. (1998). Differential thermal analysis and differential scanning calorimetry. *Handbook of thermal analysis and calorimetry, 1*, 279-361.

Halder, A., Datta, A. K., & Spanswick, R. M. (2011). Water transport in cellular tissues during thermal processing. *AIChE Journal, 57*(9), 2574-2588. doi:10.1002/aic.12465

Hanson, L. G. (2008). Is quantum mechanics necessary for understanding magnetic resonance? *Concepts in Magnetic Resonance Part A, 32*(5), 329-340.

Hatakeyama, T., Nakamura, K., & Hatakeyama, H. (1988). Determination of bound water content in polymers by DTA, DSC and TG. *Thermochimica Acta, 123*, 153-161. doi:http://dx.doi.org/10.1016/0040-6031(88)80018-2

Hatakeyama, T., Tanaka, M., Kishi, A., & Hatakeyama, H. (2012). Comparison of measurement techniques for the identification of bound water restrained by polymers. *Thermochimica Acta, 532*, 159-163. doi:http://dx.doi.org/10.1016/j.tca.2011.01.027

Hills, B. P., & Remigereau, B. (1997). NMR studies of changes in subcellular water compartmentation in parenchyma apple tissue during drying and freezing. *International Journal of Food Science & Technology, 32*(1), 51-61. doi:10.1046/j.1365-2621.1997.00381.x

Inao, S., Kuchiwaki, H., Hirai, N., Takada, S., Kageyama, N., Furuse, M., & Gonda, T. (1985). Dynamics of Tissue Water Content, Free and Bound Components, Associated with Ischemic Brain Edema. In Y. Inaba, I. Klatzo, & M. Spatz (Eds.), *Brain Edema:*

Proceedings of the Sixth International Symposium, November 7–10, 1984 in Tokyo (pp. 360-366). Berlin, Heidelberg: Springer Berlin Heidelberg.

Joardder, M. U. H., Karim, A., Brown, R. J., & Kumar, C. (2015). *Porosity : Establishing the Relationship between Drying Parameters and Dried Food Quality*: Springer.

Joardder, M. U. H., Kumar, C., & Karim, M. A. (2017). Food structure: Its formation and relationships with other properties. *Crit Rev Food Sci Nutr, 57*(6), 1190-1205. doi:10.1080/10408398.2014.971354

Karel, M., & Lund, D. B. (2003). Physical principles of food preservation: revised and expanded (Vol. 129). CRC Press.

Kerch, G., Glonin, A., Zicans, J., & Meri, R. M. (2012). A DSC study of the effect of ascorbic acid on bound water content and distribution in chitosan-enriched bread rolls during storage. *Journal of Thermal Analysis and Calorimetry, 108*(1), 73-78. doi:10.1007/s10973-011-1485-x

Khan, M. I. H., Joardder, M., Kumar, C., & Karim, M. (2016a). Multiphase porous media modelling: A novel approach of predicting food processing performance. *Critical Reviews in Food Science and Nutrition*. doi:org/10.1080/10408398.2016.1197881

Khan, M. I. H., Kumar, C., Joardder, M. U. H., & Karim, M. A. (2017a). Determination of appropriate effective diffusivity for different food materials. *Drying Technology, 35*(3), 335-346. doi:10.1080/07373937.2016.1170700

Khan, M. I. H., Wellard, R. M., Nagy, S. A., Joardder, M. U. H., & Karim, M. A. (2016b). Investigation of bound and free water in plant-based food material using NMR T_2 relaxometry. *Innovative Food Science & Emerging Technologies, 38*, 252-261. doi:10.1016/j.ifset.2016.10.015

Khan, M. I. H., Wellard, R. M., Nagy, S. A., Joardder, M. U. H., & Karim, M. A. (2017b). Experimental investigation of bound and free water transport process during drying of hygroscopic food material. *International Journal of Thermal Sciences, 117*, 266-273. doi.org/10.1016/j.ijthermalsci.2017.04.006

Kristl, M., Muršec, M., Šuštar, V., & Kristl, J. (2016). Application of thermogravimetric analysis for the evaluation of organic and inorganic carbon contents in agricultural soils. *Journal of Thermal Analysis and Calorimetry, 123*(3), 2139-2147. doi:10.1007/s10973-015-4844-1

Kuprianoff, J. (1958). Bound and free water in foods. *In: Fundamental Aspects of the Dehydration of Foodstuffs (edited by J. Kuprianoff)*. (pp. 14–23). New York: London: Society of Chemical Industry, NY: Macmillan Company.

Lee, D.J., & Lee, S. F. (1995). Measurement of bound water content in sludge: The use of differential scanning calorimetry (DSC). *Journal of Chemical Technology & Biotechnology, 62*(4), 359-365. doi:10.1002/jctb.280620408

Lee, D. J. (1996). Interpretation of bound water data measured via dilatometric technique. *Water Research, 30*(9), 2230-2232. doi:http://dx.doi.org/10.1016/0043-1354(96)00086-3

Lee, D. J., & Hsu, Y. H. (1995). Measurement of Bound Water in Sludges: A Comparative Study. *Water Environment Research, 67*(3), 310-317. doi:10.2307/25044558

Melado-Herreros, A., Muñoz-García, M.-A., Blanco, A., Val, J., Fernández-Valle, M. E., & Barreiro, P. (2013). Assessment of watercore development in apples with MRI: Effect

of fruit location in the canopy. *Postharvest Biology and Technology, 86*, 125-133. doi:http://dx.doi.org/10.1016/j.postharvbio.2013.06.030

Moser, E., Holzmueller, P., & Gomiscek, G. (1992). Liver tissue characterization by in vitro NMR: tissue handling and biological variation. *Magn Reson Med, 24*(2), 213-220.

Moser, E., Holzmueller, P., & Krssak, M. Improved estimation of tissue hydration and bound water fraction in rat liver tissue. *Magnetic Resonance Materials in Physics, Biology and Medicine, 4*(1), 55-59. doi:10.1007/bf01759780

Miyazawa, M., Pavan, M., De Oliveira, E., Ionashiro, M., & Silva, A. (2000). Gravimetric determination of soil organic matter. *Brazilian Archives of Biology and Technology, 43*(5), 475-478.

Nakamur, K., Minagaw, Y., Hatakeyam, T., & Hatakeyama, H. (2004). DSC studies on bound water in carboxymethylcellulose–polylysine complexes. *Thermochimica Acta, 416*(1–2), 135-140. doi:http://dx.doi.org/10.1016/j.tca.2003.02.002

Nakamura, K., Hatakeyama, T., & Hatakeyama, H. (1981). Studies on Bound Water of Cellulose by Differential Scanning Calorimetry. *Textile Research Journal, 51*(9), 607-613. doi:10.1177/004051758105100909

Nelson, J. H. (2003). Nuclear magnetic resonance spectroscopy: NJ: Pearson Education, Prentice Hall.

Ohno, H., Shibayama, M., & Tsuchida, E. (1983). DSC analyses of bound water in the microdomains of interpolymer complexes. Macromolecular Chemistry and Physics, 184(5), 1017-1024. doi:10.1002/macp.1983.021840513

Peyronel, M. F., & Marangoni, A. G. (2017). Differential Scanning Calorimetry, AOCS Lipid library, USA, doi: 10.21748/lipidlibrary.40884

Peishi, C., & Pei, D. C. T. (1989). A mathematical model of drying processes. *International Journal of Heat and Mass Transfer, 32*(2), 297-310. doi:http://dx.doi.org/10.1016/0017-9310(89)90177-4

Prothon, F., Ahrne, L., & Sjoholm, I. (2003). Mechanisms and prevention of plant tissue collapse during dehydration: a critical review. *Crit Rev Food Sci Nutr, 43*(4), 447-479. doi:10.1080/10408690390826581

PS., N. (2009). *Cells and Diffusion* (4th edition ed.). San Diego: CA: Elsevier, Inc.

Pallasser, R., Minasny, B., & McBratney, A. B. (2013). Soil carbon determination by thermogravimetrics. *PeerJ, 1*, e6. doi:10.7717/peerj.6

Rockland, L. B. (1969). Water activity and storage stability. *Food Technology, 23*, 1241-1251.

Rondeau, M. C., Deslis, S., Quellec, S., & Bauduin, R. (2015). Assessment of TD-NMR and Quantitative MRI Methods to Investigate the Apple Transformation Processes Used in the Cider-Making Technology. In Magnetic Resonance in Food Science (pp. 127-140). (Francesco, L. L., Capozzi, Peter S. Belton Ed. Vol. 349): The Royal society of Chemistry.

Ruan, R. R., Chen, P. L., & Almaer, S. (1999). Nondestructive Analysis of Sweet Corn Maturity Using NMR. *HortScience, 34*(2), 319-321.

Sayre, J. (1932). Methods of determining bound water in plant tissue. *Jour. Agr. Res, 44*, 669-688.

Schwartzberg, H. G. (1976). Effective heat capacities for the freezing and thawing of food. *Journal of Food Science, 41*(1), 152-156. doi:10.1111/j.1365-2621.1976.tb01123.x

Sedin, G., Bogner, P., Berenyi, E., Repa, I., Nyul, Z., & Sulyok, E. (2000). Lung Water and Proton Magnetic Resonance Relaxation in Preterm and Term Rabbit Pups: Their Relation to Tissue Hyaluronan. *Pediatr Res, 48*(4), 554-559.

Shafiur, R. (2007). Hand book of food preservation, Second edition. *CRC press, Taylor Francise, Boca Rotan, London, New York.*

Skaar, C., & Babiak, M. (1982). A model for bound-water transport in wood. *Wood Science and Technology, 16*(2), 123-138. doi:10.1007/bf00351098

Smith, J. K., & Vesilind, P. A. (1995). Dilatometric measurement of bound water in wastewater sludge. *Water Research, 29*(12), 2621-2626. doi:http://dx.doi.org/10.1016/0043-1354(95)00144-A

Srikiatden, J., & Roberts, J. S. (2007). Moisture Transfer in Solid Food Materials: A Review of Mechanisms, Models, and Measurements. *International Journal of Food Properties, 10*(4), 739-777. doi:10.1080/10942910601161672

Steele, R. (2004). *Understanding and measuring the shelf-life of food*: Woodhead Publishing.

Sulyok, E., Nyúl, Z., Bogner, P., Berényi, E., Repa, I., Vajda, Z., . . . Sedin, G. (2001). Brain Water and Proton Magnetic Resonance Relaxation in Preterm and Term Rabbit Pups: Their Relation to Tissue Hyaluronan. *Neonatology, 79*(1), 67-72.

Silva, V. M. d., Silva, L. A., Andrade, J. B. d., Veloso, M. C. d. C., & Santos, G. V. (2008). Determination of moisture content and water activity in algae and fish by thermoanalytical techniques. *Química Nova, 31,* 901-905.

Turner, I. W., Puiggali, J. R., & Jomaa, W. (1998). A Numerical Investigation of Combined Microwave and Convective Drying of a Hygroscopic Porous Material: A Study Based on Pine Wood. *Chemical Engineering Research and Design, 76*(2), 193-209. doi:http://dx.doi.org/10.1205/026387698524622

Vaclavik, V. A., & Christian, E. W. (2008). Water *Essentials of Food Science* (pp. 21-31): Springer.

Vajda, Z., Berenyi, E., Bogner, P., Repa, I., Doczi, T., & Sulyok, E. (1999). Brain adaptation to water loading in rabbits as assessed by NMR relaxometry. *Pediatr Res, 46*(4), 450-454. doi:10.1203/00006450-199910000-00015

Van de Velde, F., Grace, M. H., Esposito, D., Pirovani, M. É., & Lila, M. A. (2016). Quantitative comparison of phytochemical profile, antioxidant, and anti-inflammatory properties of blackberry fruits adapted to Argentina. *Journal of Food Composition and Analysis, 47*, 82-91. doi:http://dx.doi.org/10.1016/j.jfca.2016.01.008

Van Der Weerd, L., Claessens, M. M. A. E., Efdé, C., & Van As, H. (2002). Nuclear magnetic resonanceimaging of membrane permeability changes in plants during osmoticstress. *Plant, Cell & Environment, 25*(11), 1539-1549. doi:10.1046/j.1365-3040.2002.00934.x

van der Weerd, L., Claessens, M. M. A. E., Ruttink, T., Vergeldt, F. J., Schaafsma, T. J., & Van As, H. (2001). Quantitative NMR microscopy of osmotic stress responses in maize and pearl millet. *Journal of Experimental Botany, 52*(365), 2333-2343. doi:10.1093/jexbot/52.365.2333

Vicente, S., Nieto, A. B., Hodara, K., Castro, M. A., & Alzamora, S. M. (2012). Changes in Structure, Rheology, and Water Mobility of Apple Tissue Induced by Osmotic Dehydration with Glucose or Trehalose. *Food and Bioprocess Technology, 5*(8), 3075-3089. doi:10.1007/s11947-011-0643-2

Webber, H. H., & Dehnel, P. A. (1968). Water balance of whole animal, muscle tissue, and muscle cells in the prosobranch gastropod, Acmaea scutum. *Journal of Experimental Zoology, 168*(3), 327-335. doi:10.1002/jez.1401680304

Westbrook, C., & Roth, C. K. (2011). MRI in Practice. John Wiley & Sons.

Wheeler-Kingshott, C. A. M., Barker, G. J., Steens, S. C. A., & van Buchem, M. A. (2004). D: The Diffusion of Water *Quantitative MRI of the Brain* (pp. 203-256): John Wiley & Sons, Ltd.

Whitaker, S., & Chou, W. T. H. (1983). Drying granular porous media theory and experiment. *Drying Technology, 1*(1), 3-33. doi:10.1080/07373938308916768

Winisdorffer, G., Musse, M., Quellec, S., Devaux, M.-F., Lahaye, M., & Mariette, F. (2015). MRI investigation of subcellular water compartmentalization and gas distribution in apples. *Magnetic Resonance Imaging, 33*(5), 671-680. doi:http://dx.doi.org/10.1016/j.mri.2015.02.014

Wu, C. C., Huang, C., & Lee, D. J. (1998). Bound water content and water binding strength on sludge flocs. *Water Research, 32*(3), 900-904. doi:http://dx.doi.org/10.1016/S0043-1354(97)00234-0

Wu, L., Ogawa, Y., & Tagawa, A. (2008). Electrical impedance spectroscopy analysis of eggplant pulp and effects of drying and freezing–thawing treatments on its impedance characteristics. *Journal of Food Engineering, 87*(2), 274-280. doi:http://dx.doi.org/10.1016/j.jfoodeng.2007.12.003

Yamsaengsung, R., & Moreira, R. G. (2002). Modeling the transport phenomena and structural changes during deep fat frying: Part I: model development. *Journal of Food Engineering, 53*(1), 1-10. doi:http://dx.doi.org/10.1016/S0260-8774(01)00134-0

Zhang, M., Repo, T., Willison, J., & Sutinen, S. (1995). Electrical impedance analysis in plant tissues: on the biological meaning of Cole-Cole α in Scots pine needles. *European Biophysics Journal, 24*(2), 99-106.

Zhang MIN, S. D., Willison JHM. (1990). Electrical Impedance Analysis in Plant Tissues: Symplasmic Resistance and Membrane Capacitance in the Hayden Model. *Journal of Experimental Botany, 41*(224), 371-380.

Table

Table 1: A list of food materials with their corresponding FW, LBW, and SBW

Material	Method	FW (%)	LBW (%)	SBW (%)	Reference
Apple	NMR	9.7 ± 3.2	87.8 ± 4.2	2.5 ± 2.1	(Khan et al., 2016b)
	BIA		90–91		(Halder et al., 2011)
Pear	NMR	16 ± 2.2	80.1 ± 4.8	3.9 ± 2.0	(Khan et al., 2016b)
Kiwi	NMR	18.7 ± 3.5	76.2 ± 3.2	5.1 ± 1.8	(Khan et al., 2016b)
Nectarine	NMR	14.7 ± 3.1	80.8 ± 4.5	4.5 ± 1.9	(Khan et al., 2016b)
Apricot	NMR	13.9 ± 3.4	83.2 ± 5.2	2.9 ± 2.3	(Khan et al., 2016b)
Carrot	NMR	12.1 ± 3.2	82.7 ± 3.7	5.2 ± 2.4	(Khan et al., 2016b)
Potato	NMR	12.9 ± 2.5	81.3 ± 3.8	5.8 ± 2.1	(Khan et al., 2016b)
	BIA		95–96		(Halder et al., 2011)

Eggplant	NMR	5.5 ± 2.2	91.3 ± 4.3	3.2 ± 1.6	(Khan et al., 2016b)
	BIA		96–97		(Halder et al., 2011)
Pumpkin	NMR	16.1 ± 3.4	79.7 ± 2.2	4.2 ± 3.2	(Khan et al., 2016b)
Tomato	NMR	10.1 ± 3.3	87.6 ± 4.6	2.3 ± 2.2	(Khan et al., 2016b)
	BIA		79–85		(Halder et al., 2011)
Cucumber	NMR	10.4 ± 2.1	88.3 ± 3.2	1.3 ± 1.9	(Khan et al., 2016b)
	BIA		95–96		(Halder et al., 2011)

Figure captions

Figure 1: Cellular water distribution in plant-based food tissue (Khan et al., 2016a)

Figure 2: Cellular water distribution with material shrinkage (Joardder et al., 2015)

Figure 3: A typical DSC curve

Figure 4: (a) Current flow pattern in cellular tissue during BIA experimentation, (b) Equivalent circuit for current flow through intracellular water and intercellular water.

Figure 5: A typical Cole–Cole plot

Figure 6: Schematic diagram of BIA

Figure 7: A schematic of a typical dilatometer

Figure 8: A general trend of TG curve

Figure 1:

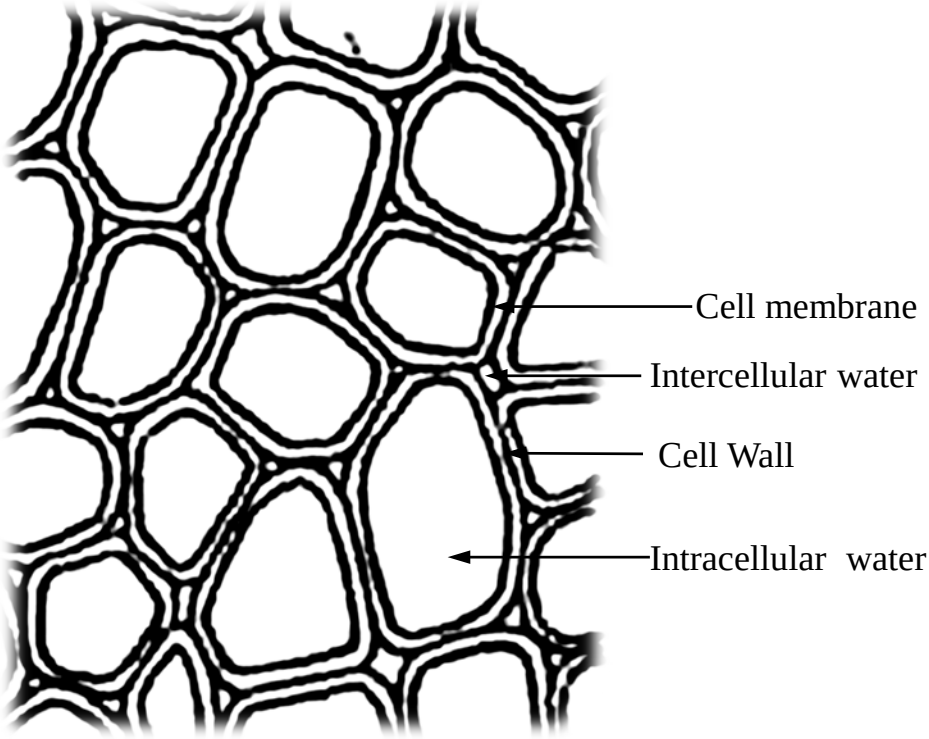
Cell membrane
Intercellular water
Cell Wall
Intracellular water

Figure 2:

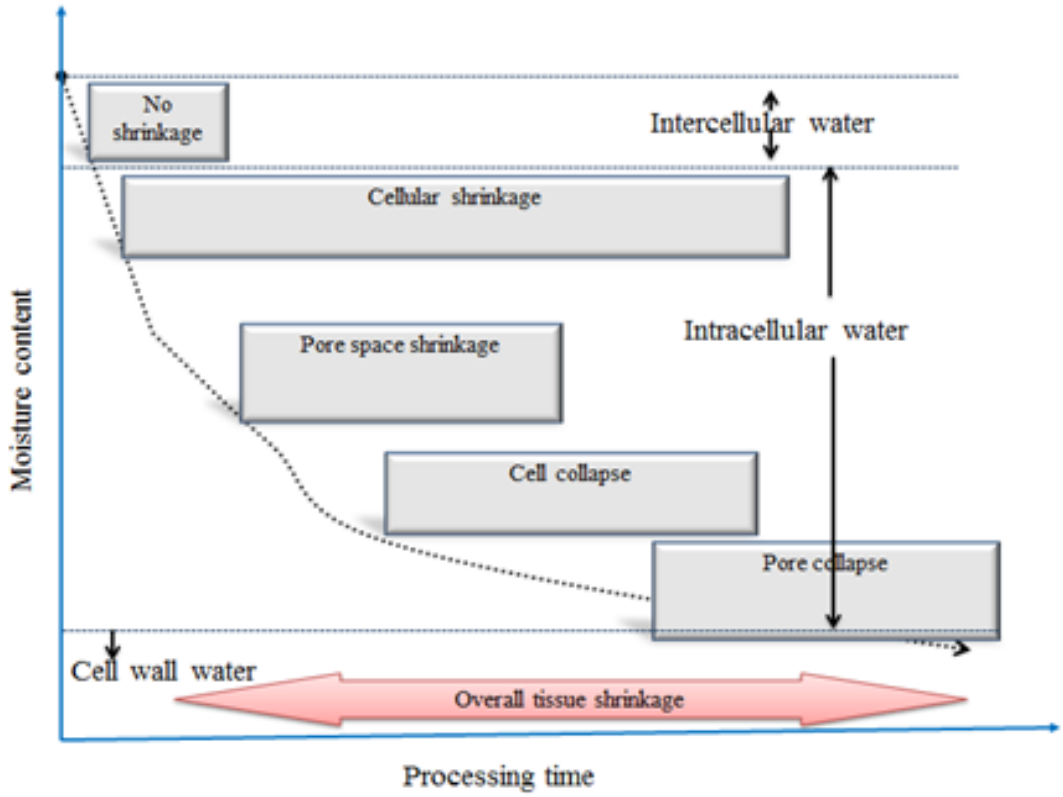
No shrinkage
Intercellular water
Cellular shrinkage
Intracellular water
Pore space shrinkage
Cell collapse
Pore collapse
Cell wall water
Overall tissue shrinkage
Moisture content
Processing time

Figure 3:

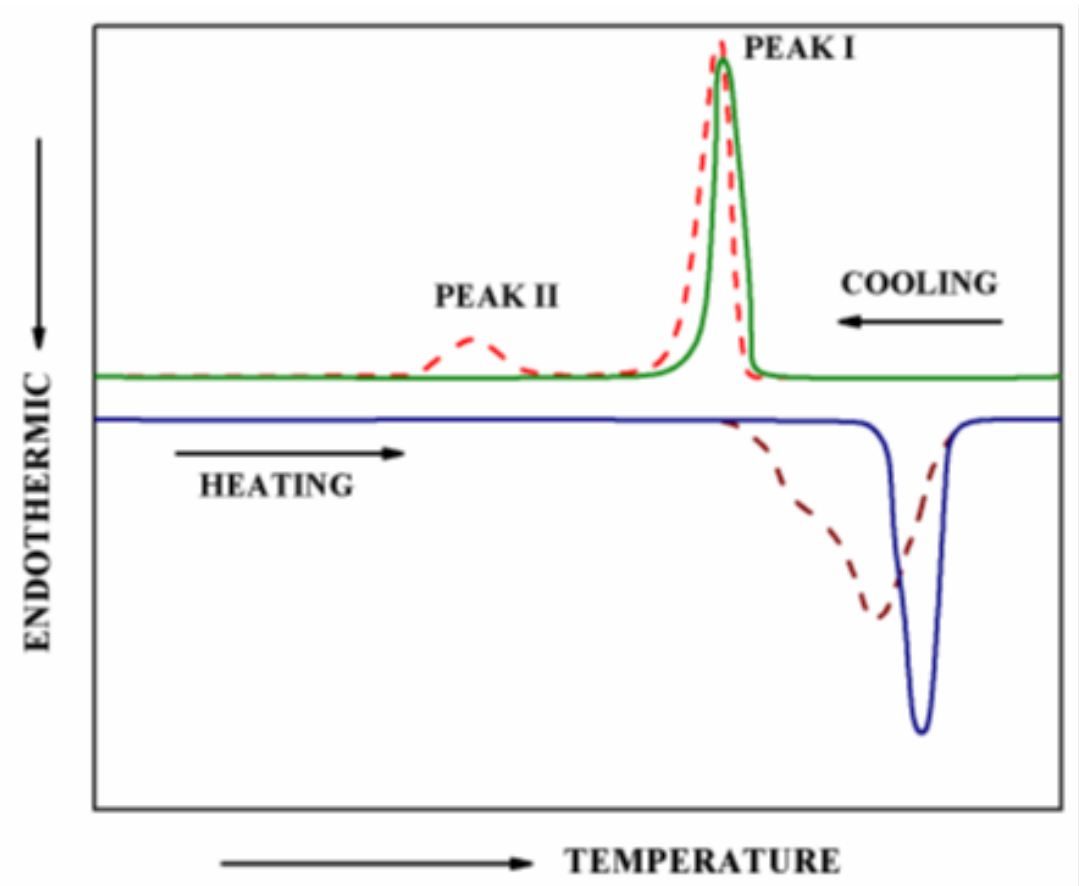

Figure 4:

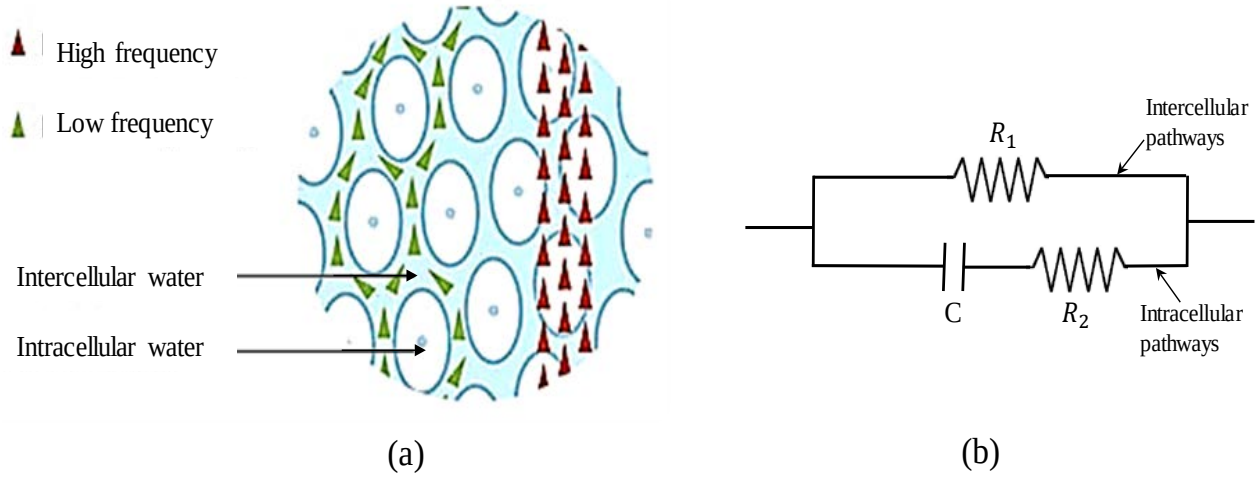
High frequency
Low frequency
Intercellular water
Intracellular water
R_1
Intercellular pathways
C
R_2
Intracellular pathways

(a) (b)

Figure 5:

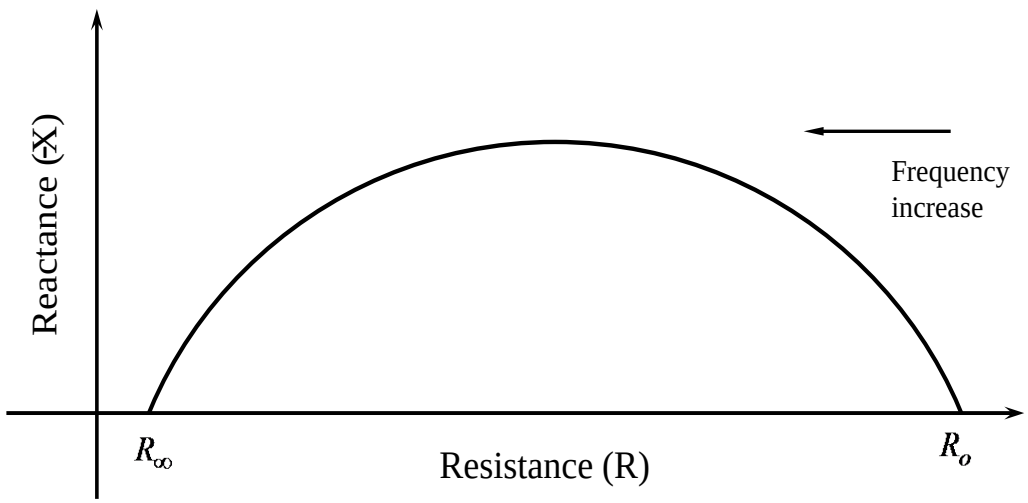

Figure 6:

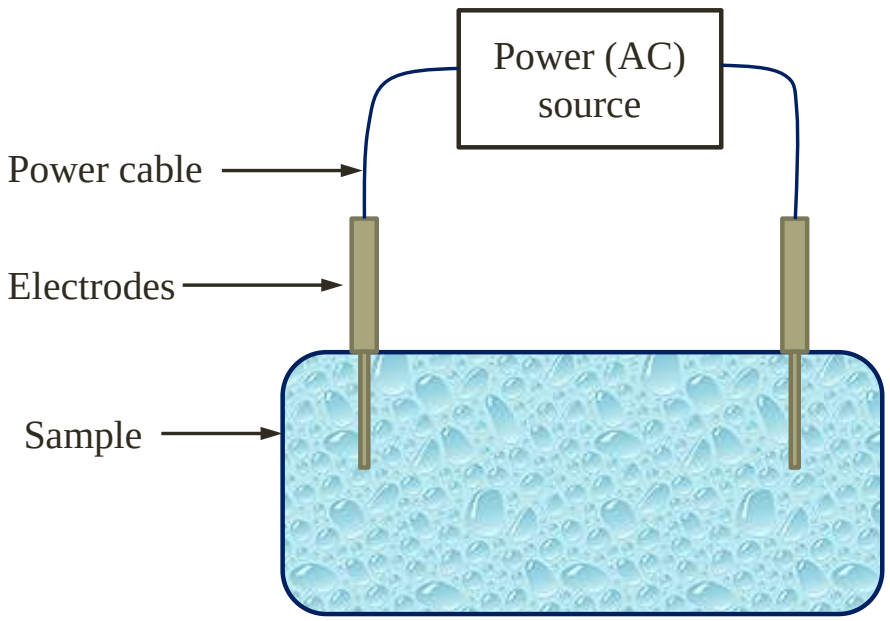

Figure 7:

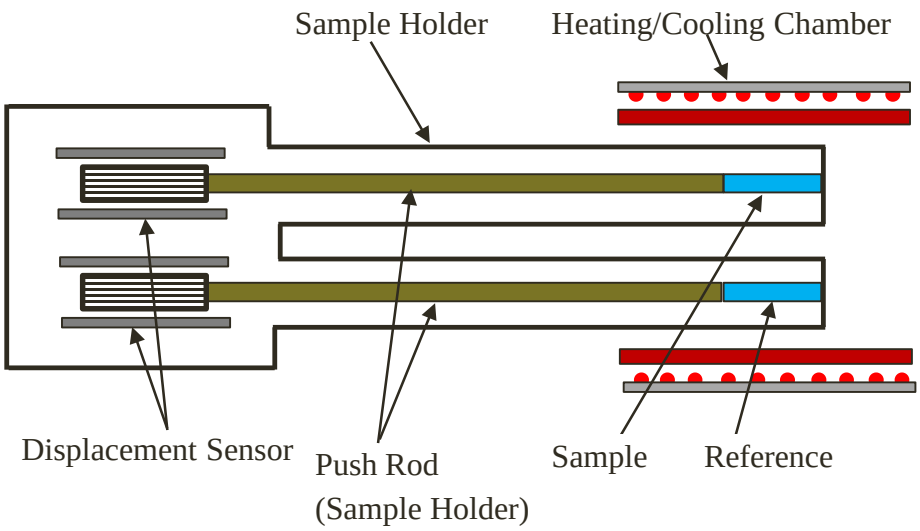
Sample Holder
Heating/Cooling Chamber
Displacement Sensor
Push Rod
(Sample Holder)
Sample
Reference

Figure 8

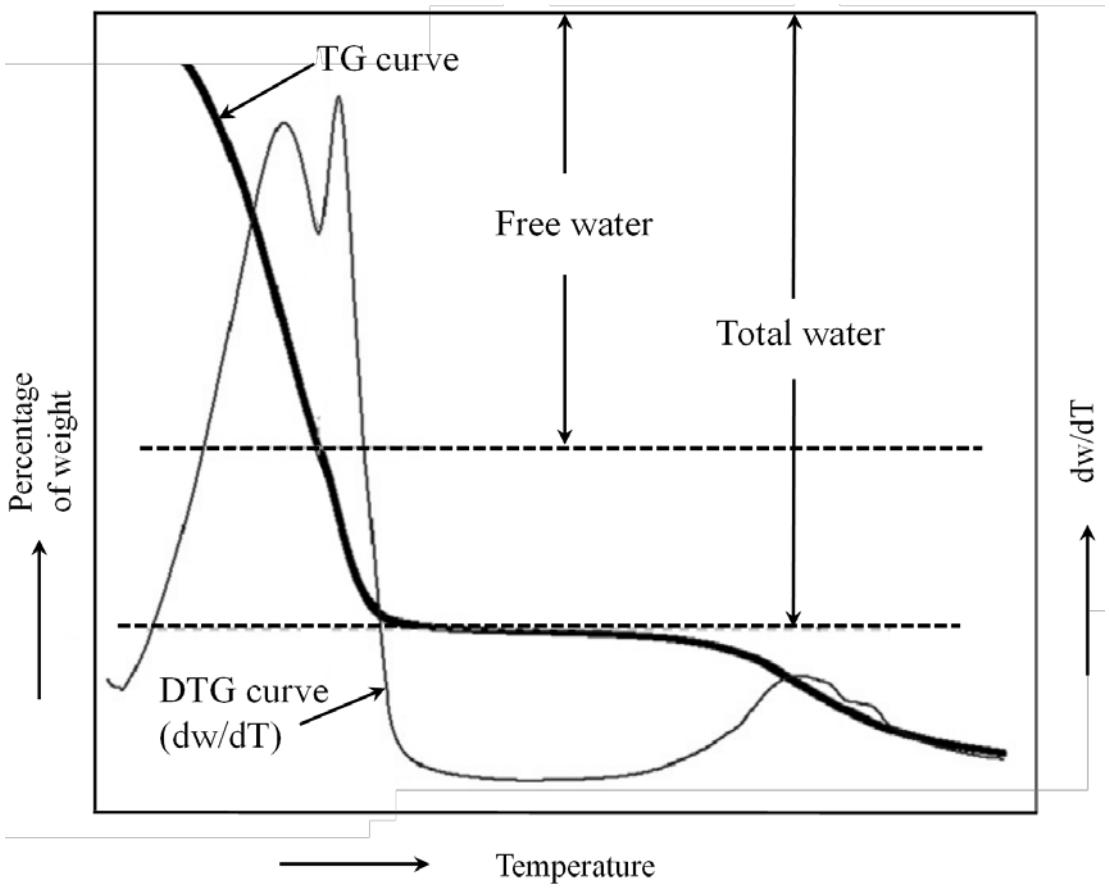
TG curve
Free water
Total water
Percentage of weight
dw/dT
DTG curve (dw/dT)
Temperature